Temporal Dynamics as Space-Growth: Kinematics and Tests with a GR Bridge

Ogaeze Onyedikachukwu Francis *

Posted Date: 28 November 2025

doi: 10.20944/preprints202511.2314.v1

Keywords: temporal Dynamics; lapse N; gravitational redshift; Shapiro delay; gravitational lensing; optical clocks; atom interferometry; dark energy

Article

Temporal Dynamics as Space-Growth: Kinematics and Tests with a GR Bridge

Ogaeze Onyedikachukwu Francis

Independent Research, Delta, Nigeria; ogaezefrancis884@gmail.com

Abstract

We formulate *Temporal Dynamics* (TD), a clock-first description in which a universal space–growth speed $S(t)$ sets the causal baseline and a dimensionless slow–time field $\Delta T(\mathbf{x}, t)$ encodes local rate loss. In the quasistatic, weak field we use a single scalar to control kinematics and optics: $\mathbf{g} = -(S^2/2)\nabla\Delta T$ and $n(\mathbf{x}) = 1/\sqrt{1-\Delta T(\mathbf{x})}$. With the *Normalization Axiom* $S \equiv c$ and the identification $N^2 = 1 - \Delta T$, TD reproduces GR's tested content (Newtonian limit, gravitational redshift, Shapiro delay, light deflection, and standard GW degrees of freedom) without introducing a new propagating mode. Horizons occur at $\Delta T \to 1$, fixing the global mass–size calibration $D_{\mathrm{BH}} = 4GM/c^2$. The source law uses the GR weak-field "active density" $\rho + (p_x + p_y + p_z)/c^2$, cleanly separating EM *propagation* (via n) from *sourcing* (via stresses). Allowing a tiny homogeneous clock drift $\varepsilon(t) = \dot{S}/c$ yields an effective $\Lambda(t) = 3\varepsilon(t)^2/c^2$, a one-parameter extension of ΛCDM with distances $E^2(z)$ modified by $(1+z)^{2p}$. We outline a falsifiable program: map $\Delta T(\mathbf{x})$ with clock networks and atom interferometers, test the optical dictionary on engineered links and lensing, and fit the cosmological parameter p with SN Ia, BAO, and $H(z)$, cross-checking growth and the turnaround scale $r_* = (GM/\varepsilon^2)^{1/3}$.

Keywords: temporal Dynamics; lapse N; gravitational redshift; Shapiro delay; gravitational lensing; optical clocks; atom interferometry; dark energy

---

1. Introduction

General Relativity (GR) describes gravity extraordinarily well in terms of spacetime geometry and has passed a wide range of precision tests[1–3]. In this paper we present a native formulation of *Temporal Dynamics (TD)* in which a universal *space–growth clock* produces adjacency. The clock has baseline speed $S(t)$ ($\mathrm{m\,s^{-1}}$), and mass–energy creates a dimensionless *slow–time field* $\Delta T(\mathbf{x}, t) \in [0, 1)$ that locally taxes the clock. Kinematics and optics then follow from this single field: bodies fall down gradients of ΔT, and light propagates as if vacuum had an index $n(\mathbf{x}) = 1/\sqrt{1-\Delta T(\mathbf{x})}$, reproducing the standard weak-field lensing picture[4]. (For TD background and motivation see Ref. [5].)

Thesis (cause → representation).

When the baseline is *frozen* to a constant $S \equiv c$ and the ADM lapse is identified by

$$N^2 \;=\; 1 - \Delta T, \tag{1}$$

TD reproduces GR's tested content (Newtonian limit, gravitational redshift, Shapiro delay, lensing, and gravitational waves) without introducing new degrees of freedom[1,6–13]. In this sense, GR is the *representation* of a clocked universe under a frozen baseline; TD supplies the *cause*. Allowing a tiny uniform drift $\varepsilon(t) = \dot{S}/c$ yields an effective dark–energy term

$$\Lambda(t) \;=\; \frac{3\,\varepsilon(t)^2}{c^2}, \tag{2}$$

which reduces to GR+Λ when ε is constant and vanishes when $\varepsilon = 0$; observationally, a constant term is consistent with supernovae and BAO evidence for late-time acceleration[14–16].

 doi:10.20944/preprints202511.2314.v1

Operational content.

The field ΔT is defined by clock comparisons: for static observers $d\tau = N\,dt$ with N from (1). Classical and modern redshift tests (Mössbauer, optical clocks, satellite clocks) implement precisely this comparison[17–21]. With normal matter and appropriate boundary conditions (asymptotic flatness), $0 \le \Delta T < 1$ outside horizons. The endpoint $\Delta T \to 1$ marks a *black boundary* (lapse $N \to 0$); it is distinct from the "pre-clock" state $S = 0$, in which spacetime is not yet operationally defined.

Minimal laws used throughout.

In the quasistatic, weak-field regime TD uses:

$$v(\mathbf{x},t) \;=\; S(t)\,\Delta T(\mathbf{x},t), \tag{3}$$

$$\mathbf{g}(\mathbf{x},t) \;=\; -\frac{S(t)^2}{2}\,\nabla\Delta T(\mathbf{x},t), \tag{4}$$

$$\nabla^2\Delta T \;=\; \frac{8\pi G}{c^2}\left(\rho + \frac{p_x+p_y+p_z}{c^2}\right) \quad \text{(active density)}, \tag{5}$$

$$n(\mathbf{x}) \;=\; \frac{1}{\sqrt{1-\Delta T(\mathbf{x})}} \;\approx\; 1 + \tfrac{1}{2}\Delta T(\mathbf{x}) \quad (\Delta T \ll 1). \tag{6}$$

The source combination in (5) (pressures gravitate) is the standard weak-field GR result[22]. With the weak-field identification $\Delta T(r) \approx 2GM/(c^2 r)$ and the *Normalization Axiom* $S \equiv c$, Eq. (4) gives exactly Newton's law. The *horizon calibration* $\Delta T = 1$ sets the black-boundary diameter

$$D_{\mathrm{BH}} \;=\; \frac{4G}{c^2}\,M, \tag{7}$$

consistent with the Schwarzschild limit[2,3] and explicitly used in the TD $\leftrightarrow$GR bridge[13].

What this paper does (and does not) claim.

- **Cause:** We posit a physical clock $S(t)$ that produces adjacency; ΔT is a measurable field that encodes local slow–time.
- **Kinematics & optics from one scalar:** Eqs. (3)–(6) unify free-fall, redshift, Shapiro delay, and lensing[1,4,5,8].
- **Bridge to GR:** Setting $S = c$ and using (1) reproduces standard tests and leaves the constraint structure and radiative degrees of freedom unchanged[1,6,7,13]. The full action-level mapping and degree-of-freedom count are provided in the bridge note[13].
- **TD-specific handle:** A tiny uniform drift $\varepsilon(t)$ (clock drift) appears as $\Lambda(t)$ in (2) and leads to the turnaround scale $r_* = (GM/\varepsilon^2)^{1/3}$ separating bound from unbound flow.
- **No new scalar graviton:** We do *not* add a propagating scalar gravitational mode; ΔT is a representation of the lapse, not an extra DoF, consistent with GW observations[11,12].

Scope and structure.

Section 2 states the axioms and normalizations (including the necessity of $S \equiv c$ in our epoch for empirical calibration). Section 3 gives an operational definition of ΔT and its domain of validity. Section 4 derives Newton's law and collects the TD$\to$observable dictionary. Section 5 treats optical tests via the index $n(\Delta T)$. Section 6 discusses horizons and the mass–size law. Section 7 incorporates pressures in sourcing ΔT and clarifies why mass typically produces steeper local slow–time gradients than radiation. Section 8 points to the GR bridge note. Section 9 places classical electromagnetism on a TD background (propagation vs. sourcing). Section 10 lists quantum-ready observables (clocks and interferometers). Section 11 treats cosmology (clock drift, genesis picture, and key scales). Section 12 outlines laboratory and astronomical tests; Section 13 addresses common objections; Section 14 states limitations; Section 15 concludes. A compact notation reference is given in Appendix H, Table H.

 doi:10.20944/preprints202511.2314.v1

2. Axioms and Normalization

This section states the primitive quantities and the minimal laws of Temporal Dynamics (TD). We keep the presentation quasistatic and weak field unless stated otherwise; dynamical refinements can be added later without changing the calibration logic. A compact summary of axioms and references is given in Table 1. A schematic of the relations between primitives, kinematics, optics, and calibration is shown in Figure 1; the horizon calibration is illustrated in Figure 2.

2.1. Primitives and Units

Axiom A (Clock / space–growth). There exists a baseline space–growth speed $S(t)$ ($\mathrm{m\,s^{-1}}$) representing the universal production of adjacency per unit cosmic time. In the *bridge regime* it will be frozen to a constant (§2.6).

Axiom B (Slow–time field). A dimensionless scalar $\Delta T(\mathbf{x}, t) \in [0, 1)$ encodes the local slow–down of the clock. For static observers the proper time satisfies

$$d\tau \;=\; N\,dt, \qquad N^2 \;=\; 1 - \Delta T, \tag{8}$$

so ΔT is literally the fraction of baseline rate lost at $(\mathbf{x}, t)$. (Here N is the ADM lapse[6,7]; see also the TD $\to$GR bridge[13].)

2.2. Kinematics and Gravity (Quasistatic)

Axiom C (Kinematics). The peculiar speed of a test body relative to the baseline is

$$v(\mathbf{x}, t) \;=\; S(t)\,\Delta T(\mathbf{x}, t). \tag{9}$$

Axiom D (Gradient law for gravity). In a quasistatic field the gravitational acceleration is

$$\mathbf{g}(\mathbf{x}, t) \;=\; -\frac{S(t)^2}{2}\,\nabla \Delta T(\mathbf{x}, t). \tag{10}$$

2.3. Sourcing by Stress–Energy (Active Density)

Axiom E (Poisson law, weak/static). Outside sources and for $|\Delta T| \ll 1$ with slow time variation,

$$\nabla^2 \Delta T \;=\; \frac{8\pi G}{c^2}\left(\rho + \frac{p_x + p_y + p_z}{c^2}\right) \;\equiv\; \frac{8\pi G}{c^2}\,\rho_{\text{active}}. \tag{11}$$

Here ρ is energy density ($\mathrm{J\,m^{-3}}/c^2$), p_i are principal pressures, and ρ_{active} is the standard weak–field GR combination ("pressures gravitate")[1,22]. Electromagnetic fields contribute via $u_{\text{EM}} = \frac{1}{2}(\varepsilon_0 E^2 + B^2/\mu_0)$ and $\rho_{\text{EM}} = u_{\text{EM}}/c^2$; see also the TD EM development[23].

2.4. Optics: Index of Time

Axiom F (Propagation of light). Light propagates as if vacuum had an effective index

$$n(\mathbf{x}) \;=\; \frac{1}{\sqrt{1 - \Delta T(\mathbf{x})}} \;\approx\; 1 + \tfrac{1}{2}\,\Delta T(\mathbf{x}) \quad (\Delta T \ll 1), \tag{12}$$

which reproduces gravitational redshift, Shapiro delay, and weak lensing directly from ΔT via Fermat's principle/optical metric[1,4,5,8,23].

 doi:10.20944/preprints202511.2314.v1

2.5. Horizon Calibration

Axiom G (Black boundary). The surface $\Delta T = 1$ defines a black boundary (static lapse $N \to 0$). Matching to the Schwarzschild scale fixes the global calibration constant

$$D_{\mathrm{BH}} = \frac{4G}{c^2} M \equiv k\, M, \qquad k = \frac{4G}{c^2}. \tag{13}$$

Equivalently, the diameter equals $2r_s$ with $r_s = 2GM/c^2$[2,3]; this identity is central in the TD bridge[13]. See Figure 2.

2.6. Normalization and Necessity of $S \equiv c$

The empirical calibrations used throughout are:

$$\Delta T(r) \approx \frac{2GM}{c^2 r} \quad \text{(weak field outside a mass)}, \qquad D_{\mathrm{BH}} = \frac{4G}{c^2} M. \tag{14}$$

Inserting the first of (14) into the gradient law (10) fixes the overall scale:

$$\left|\mathbf{g}(r)\right| = \frac{S^2}{c^2} \frac{GM}{r^2}. \tag{15}$$

Normalization Lemma. *To recover Newton's law exactly from Eq. (15), the baseline must satisfy $S = c$.* See Appendix B and the bridge note[13].

Comment. Choosing a constant $S \neq c$ while keeping (14) would mis-scale gravity by S^2/c^2. One could re-define the calibrations with $c \to S$, but that is merely a change of symbols. In the realized epoch we therefore impose the **Normalization Axiom**:

$$S \equiv c \quad \text{(current epoch)}. \tag{16}$$

2.7. Domain and Boundary Conditions (Summary)

We adopt asymptotic flatness so that $N \to 1$ and $\Delta T \to 0$ at spatial infinity. For normal (positive) energy densities and static exteriors, the elliptic maximum principle implies

$$0 \leq \Delta T(\mathbf{x}) < 1 \qquad \text{(outside horizons)}. \tag{17}$$

The endpoint $\Delta T \to 1$ marks a horizon (black boundary). The *pre-clock* boundary $S = 0$ is distinct: before the clock turns on, neither t, $d\tau$, nor ΔT are operationally defined[2,3]. A full *operational* construction of ΔT from clock networks is provided next (Section 3).

Table 1. TD axioms and key formulas. Each axiom is referenced in-text; standard GR/optics references are cited where appropriate.

Axiom	Content	Key relation / cite
A	Baseline clock $S(t)$	Normalization Axiom $S \equiv c$
B	Slow–time ΔT & lapse	$N^2 = 1 - \Delta T$ (8); ADM[6,7]
C	Kinematics	$v = S\,\Delta T$ (9)
D	Gravity (gradient law)	$\mathbf{g} = -(S^2/2)\nabla \Delta T$ (10)
E	Source law (weak/static)	Eq. (11); [1,22]
F	Optics (index of time)	$n = 1/\sqrt{1 - \Delta T}$ (12); [4,8]
G	Horizon calibration	$D_{\mathrm{BH}} = 4GM/c^2$ (13); [2,3]

 doi:10.20944/preprints202511.2314.v1

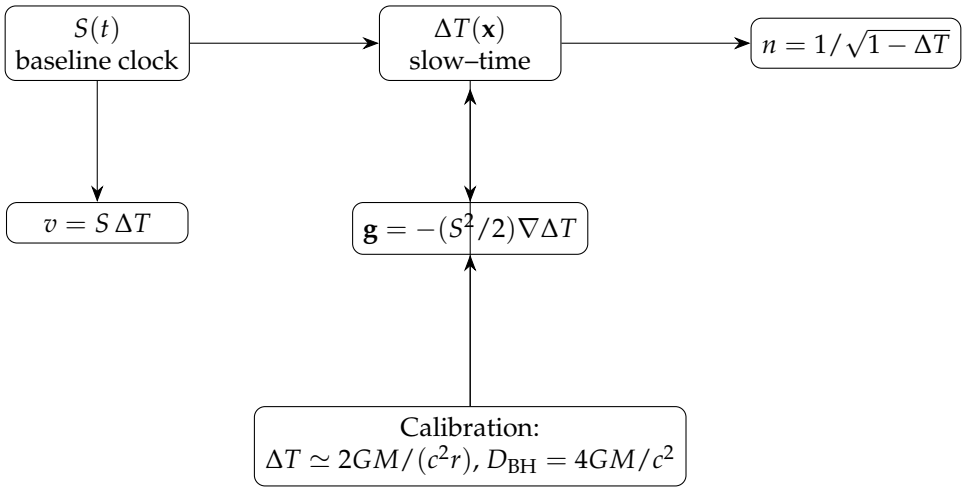

Figure 1. Schematic of TD primitives and observables. Baseline $S(t)$ and slow–time field $\Delta T(\mathbf{x})$ feed kinematics $(v, \mathbf{g})$ and optics (n); calibration enters through $\Delta T \simeq 2GM/(c^2 r)$ and $D_{\mathrm{BH}} = 4GM/c^2$. This diagram summarizes Eqs. (9)–(12) and (14).

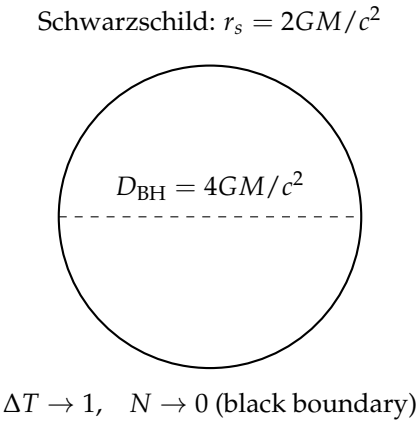

Figure 2. Horizon calibration. The black boundary is $\Delta T \to 1$ ($N \to 0$). Matching to the Schwarzschild solution sets $D_{\mathrm{BH}} = 4GM/c^2$ (Eq. (13)), used as a single global calibration across the framework[2,3,13].

3. Operational Definition of ΔT

This section defines $\Delta T(\mathbf{x})$ purely from clock comparisons and signal transfer, tying the field to observables and keeping it coordinate–independent. We assume quasistatic conditions (negligible frame dragging at the measurement scale) and work in the exterior of horizons.

3.1. Clocks, Rates, and the Lapse

For static observers, proper time satisfies $d\tau = N\,dt$ with $N^2 = 1 - \Delta T$ (Eq. (8); N is the ADM lapse[6,7]). Consider two co–stationary clocks at events A and B connected by a phase–coherent link (optical fiber, microwave, or free–space two–way). Let ν_A and ν_B be the locally measured transition frequencies of identical standards. In the quasistatic limit,

$$\frac{\nu_B}{\nu_A} = \frac{N_B}{N_A} = \sqrt{\frac{1-\Delta T_B}{1-\Delta T_A}}. \tag{18}$$

Equation (18) defines *differences* of ΔT from clock data. When $\Delta T \ll 1$,

$$\frac{\nu_B - \nu_A}{\nu_A} \approx -\tfrac{1}{2}\big(\Delta T_B - \Delta T_A\big). \tag{19}$$

 doi:10.20944/preprints202511.2314.v1

This relation is the basis of gravitational redshift tests from Mössbauer/Pound–Rebka to modern optical clocks and satellites[17–21].

3.2. Local Gradients from Frequency Maps

A dense network of clocks provides a scalar field $\nu(\mathbf{x})$ whose spatial gradient yields $\nabla\Delta T$ directly. Taking the differential of Eq. (18) and linearizing,

$$\nabla\Delta T(\mathbf{x}) \;\approx\; -\,2\,\nabla\ln\nu(\mathbf{x}). \tag{20}$$

Combined with the TD gradient law (Eq. (10)) this gives a fully operational expression for the gravitational acceleration:

$$\boxed{\mathbf{g}(\mathbf{x}) \;=\; -\frac{c^2}{2}\,\nabla\Delta T(\mathbf{x}) \;\approx\; c^2\,\nabla\ln\nu(\mathbf{x})} \qquad \text{(quasistatic, weak field).} \tag{21}$$

In words: the *spatial derivative of the log clock frequency* equals the local gravitational field divided by c^2. This is coordinate–free and depends only on what co–located observers read from their instruments. A schematic of the mapping pipeline is shown in Figure 3.

3.3. Reconstructing ΔT (Dirichlet/Neumann)

Absolute values follow by fixing a boundary condition. With asymptotic flatness $\Delta T \to 0$ at large radius, one can integrate Eq. (20) along any path from infinity to $\mathbf{x}$,

$$\Delta T(\mathbf{x}) \;\approx\; -\,2\int_{\infty}^{\mathbf{x}} \nabla\ln\nu\cdot d\boldsymbol{\ell}, \qquad (\Delta T \ll 1). \tag{22}$$

On finite laboratory domains, either

1. *Dirichlet:* set ΔT on a reference surface (e.g., from an exterior model) and integrate inward, or
2. *Neumann:* measure $\mathbf{n}\cdot\nabla\Delta T$ (via vertical clock gradients) on the boundary and solve the Poisson problem

$$\nabla^2\Delta T \;=\; \frac{8\pi G}{c^2}\,\rho_{\text{active}} \quad \text{with} \quad \begin{cases} \Delta T|_{\partial\Omega} \text{ (Dirichlet)} \\ \mathbf{n}\cdot\nabla\Delta T|_{\partial\Omega} \text{ (Neumann)} \end{cases} \tag{23}$$

for the region Ω of interest (cf. Eq. (11)).

3.4. Practical Measurement Protocol

1. **Clock grid.** Deploy identical (or cross–calibrated) clocks at positions $\{\mathbf{x}_i\}$; record $\nu(\mathbf{x}_i)$ with traceable time transfer (two–way fiber/microwave or common–view)[24].
2. **Frequency ratios.** Compute $\nu(\mathbf{x}_j)/\nu(\mathbf{x}_i)$ for neighboring pairs to suppress common–mode noise.
3. **Gradient estimation.** Fit $\nabla\ln\nu$ over local baselines (finite–difference or regression); propagate uncertainties from the Allan deviations of the clocks and links.
4. **Field and map.** Use Eq. (21) to recover $\mathbf{g}(\mathbf{x})$; integrate Eq. (22) (with boundary condition) to obtain $\Delta T(\mathbf{x})$.
5. **Source inversion (optional).** Insert the reconstructed ΔT into Eq. (11) to estimate ρ_{active} (resolution limited by noise and boundary modeling). The end-to-end steps are summarized in Table 2

 doi:10.20944/preprints202511.2314.v1

Table 2. Operational pipeline for mapping ΔT. The inputs are instrument readings and transfer links; outputs are the field, its gradient, and (optionally) source inversions.

Step	Input/Method	Primary output
Clock grid	$\nu(\mathbf{x}_i)$, stable links[24]	Frequency field $\nu(\mathbf{x})$
Ratios	Neighbor pairs	Common–mode rejection
Gradients	Fit $\nabla \ln \nu$	$\nabla \Delta T \approx -2\nabla \ln \nu$ (Eq. (20))
Field	Path integral / PDE	$\Delta T(\mathbf{x})$ (Eqs. (22), (23))
Gravity	Eq. (21)	$\mathbf{g}(\mathbf{x}) = c^2 \nabla \ln \nu$
Source (opt.)	Eq. (11)	$\rho_{\text{active}}(\mathbf{x})$

3.5. Domain, Validity, and Limits

- **Range.** With normal matter and exterior boundary conditions, $0 \leq \Delta T < 1$ (Eq. (17)). The endpoint $\Delta T \to 1$ corresponds to a black boundary where $N \to 0$ and static observers cease to exist.
- **Quasistatic assumption.** Eqs. (18)–(21) presume negligible time variation during measurement windows and co–stationary worldlines. Rotational frame effects (shift N^i) can be included by standard kinematic corrections if needed.
- **Independence of coordinates.** The construction uses only ratios of locally measured frequencies and spatial differences taken along a physical baseline; coordinates are bookkeeping for plotting and PDE solvers.
- **Laboratory scale.** In Earth's field, vertical clock pairs separated by Δh satisfy

$$\frac{\Delta \nu}{\nu} \approx \frac{g\,\Delta h}{c^2} \approx -\tfrac{1}{2}\,\Delta(\Delta T), \tag{24}$$

consistent with Eq. (21). Modern optical clocks already resolve the $\sim 10^{-16}/\text{m}$ level needed for meter–scale mapping[19].

3.6. Horizon and Pre–Clock Distinctions

Approaching a horizon, $N \to 0$ and $\nu_B/\nu_A \to 0$ for a static link crossing outward to inward (Eq. (18)); $\Delta T \to 1^-$. By contrast, in the *pre–clock* state $S = 0$ no operational time or space exists, and ΔT is undefined. The two limits must not be conflated.

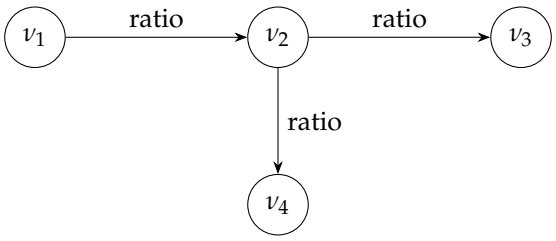

Ratios $\Rightarrow \nabla \ln \nu \Rightarrow \nabla \Delta T$ (Eq. (20))
and $\mathbf{g} = c^2 \nabla \ln \nu$ (Eq. (21))

Figure 3. Clock-network mapping of ΔT. Nodes (clocks) are connected by phase–coherent links. Frequency ratios determine $\nabla \ln \nu$, which yields $\nabla \Delta T$ via Eq. (20); integrating gives $\Delta T(\mathbf{x})$ (Eqs. (22), (23)), and Eq. (21) gives $\mathbf{g}(\mathbf{x})$.

4. Kinematics and Gravity from ΔT

This section shows how TD turns the slow–time field ΔT into motion and standard observables. We work in the quasistatic, weak–field regime and use the normalization $S \equiv c$ from Eq. (16).

 doi:10.20944/preprints202511.2314.v1

4.1. Newton's Law from the Gradient of ΔT

Outside an isolated mass M, the weak–field identification is

$$\Delta T(r) \approx \frac{2GM}{c^2 r}, \qquad (r \text{ outside the source}). \tag{25}$$

Taking the spatial gradient and using the TD gradient law (Eq. (10)) yields

$$\left|\nabla \Delta T(r)\right| = \frac{2GM}{c^2 r^2}, \qquad \left|\mathbf{g}(r)\right| = \frac{c^2}{2}\left|\nabla \Delta T(r)\right| = \frac{GM}{r^2}, \tag{26}$$

with $\mathbf{g}$ directed *inward* (toward decreasing r). Thus TD reproduces Newton's inverse–square law exactly in the weak field, consistent with standard GR[1–3].

Numerical check (Earth).

With $G = 6.67430 \times 10^{-11}\,\mathrm{m^3\,kg^{-1}\,s^{-2}}$, $M_\oplus = 5.972 \times 10^{24}\,\mathrm{kg}$, $R_\oplus = 6.371 \times 10^{6}\,\mathrm{m}$, Eq. (26) gives

$$g_\oplus = \frac{GM_\oplus}{R_\oplus^2} \approx 9.82\,\mathrm{m\,s^{-2}}.$$

At the surface, the slow–time fraction is tiny but finite:

$$\Delta T(R_\oplus) \approx \frac{2GM_\oplus}{c^2 R_\oplus} \sim 1.4 \times 10^{-9}.$$

4.2. TD $\to$ Observables: the Minimal Dictionary

In TD the same scalar ΔT governs mechanical and optical effects. To leading order in $\Delta T \ll 1$: The minimal dictionary used throughout is summarized in Table 3.

Table 3. Minimal TD$\to$observable dictionary in the quasistatic, weak–field regime ($\Delta T \ll 1$) with the Normalization Axiom $S \equiv c$. The Shapiro delay and lensing expressions reduce to the standard GR results [4,8].

Quantity	**TD expression (weak field)**
Gravitational acceleration	$\mathbf{g}(\mathbf{x}) = -\frac{c^2}{2}\nabla \Delta T(\mathbf{x})$
Gravitational redshift	$\frac{\nu_B}{\nu_A} = \sqrt{\frac{1-\Delta T_B}{1-\Delta T_A}} \approx 1 - \frac{1}{2}(\Delta T_B - \Delta T_A)$
Shapiro time delay	$\Delta t_{\text{Shapiro}} \approx \frac{1}{2c}\int_\Gamma \Delta T\, ds$ [8]
Light deflection (small angle)	$\hat{\alpha} \approx \frac{1}{2}\int \nabla_\perp \Delta T\, ds$ [4]
Effective index of vacuum	$n(\mathbf{x}) = \frac{1}{\sqrt{1-\Delta T(\mathbf{x})}} \approx 1 + \frac{1}{2}\Delta T(\mathbf{x})$

These expressions reproduce the standard weak–field GR results[1] when $\Delta T(r) = 2GM/(c^2 r)$ is used for an isolated mass.

4.3. Quick Numerical Checks (Optics and Timing)

(a) Gravitational redshift over $\Delta h = 1\,\mathrm{m}$ on Earth.

From Eq. (18) (or Eq. (21) in Sec. 3), one finds

$$\frac{\Delta \nu}{\nu} \approx \frac{g\,\Delta h}{c^2} \approx \frac{9.81 \times 1}{(2.998 \times 10^8)^2} \sim 1.1 \times 10^{-16},$$

matching state–of–the–art clock comparisons[19].

 doi:10.20944/preprints202511.2314.v1

(b) Shapiro delay for a ray grazing the Sun (one–way).

For a line of sight from Earth to a receiver at ~ 1 AU with impact parameter $b \simeq R_\odot$, the path integral with Eq. (25) gives the standard logarithmic result

$$\Delta t_{\text{Shapiro}} \approx \frac{2GM_\odot}{c^3} \ln\left(\frac{4r_E r_R}{b^2}\right) \sim 1.2 \times 10^{-4}\,\text{s},$$

i.e. $\sim 120\,\mu$s one–way ($\sim 240\,\mu$s two–way)[8,9].

(c) Light deflection by the Sun at the limb.

With $b = R_\odot$, the small–angle integral yields

$$\hat{\alpha} = \frac{4GM_\odot}{c^2 R_\odot} \approx 1.75 \text{ arcseconds},$$

the classic Eddington value[10].

4.4. Ray Picture (Index of Time): A Visual

Figure 4 sketches rays in the effective medium $n(\mathbf{x}) = (1 - \Delta T)^{-1/2}$. Gradients of n bend rays toward the mass (deflection), while the excess optical path gives the time delay (Shapiro) — both are simply functionals of ΔT along the path[4].

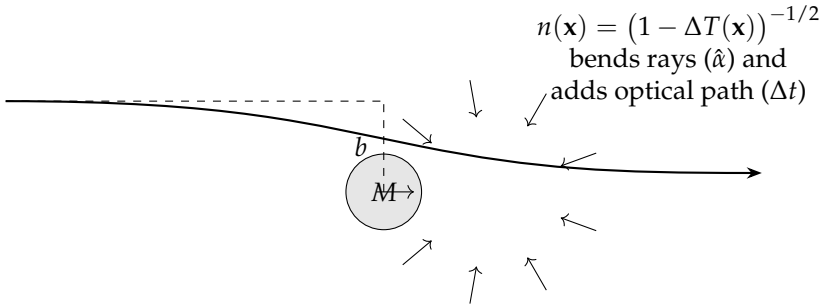

Figure 4. Ray picture in the index-of-time medium. Gradients of $n(\mathbf{x})$ (set by ΔT) deflect light and produce the Shapiro delay; both recover the standard GR values in the weak field.

4.5. Remarks

- The dictionary above follows directly from Eqs. (10) and (12); no additional structure is assumed.
- For extended sources or nonradial paths, replace $\Delta T(r)$ by the appropriate solution of Eq. (11) and evaluate the line integrals numerically (ray tracing in $n(\mathbf{x})$)[4].
- Beyond the weak/quasistatic regime, the same observables can be phrased in terms of the full $N^2 = 1 - \Delta T$ with shift and spatial metric where needed; results coincide with GR in the bridge limit[1].

5. Optical Tests via the Index $n(\Delta T)$

In TD a static, weak field acts like an isotropic medium with effective refractive index

$$n(\mathbf{x}) = \frac{1}{\sqrt{1 - \Delta T(\mathbf{x})}} \approx 1 + \tfrac{1}{2}\Delta T(\mathbf{x}) \qquad (\Delta T \ll 1), \tag{27}$$

cf. Eq. (12). Light rays extremize the coordinate travel time

$$T[\Gamma] = \frac{1}{c}\int_\Gamma n(\mathbf{x})\, ds, \tag{28}$$

which is Fermat's principle in the TD/optical-metric picture (equivalent to the weak-field GR optical metric[1,4]). All standard optical tests follow from (27)–(28).

 doi:10.20944/preprints202511.2314.v1

5.1. Gravitational Redshift

For static observers, proper time satisfies $d\tau = N\,dt$ with $N^2 = 1 - \Delta T$ (Eq. (8)). Identical clocks at A and B compare as

$$\frac{\nu_B}{\nu_A} = \frac{N_B}{N_A} = \sqrt{\frac{1-\Delta T_B}{1-\Delta T_A}} \approx 1 - \tfrac{1}{2}(\Delta T_B - \Delta T_A), \tag{29}$$

reproducing the weak-field gravitational redshift[17–21].[1]

5.2. Shapiro Time Delay

Given (28), the extra (one-way) travel time relative to an unperturbed straight path is

$$\Delta t_{\text{Shapiro}} = \frac{1}{c}\int_\Gamma (n-1)\,ds \approx \frac{1}{2c}\int_\Gamma \Delta T(\mathbf{x})\,ds, \tag{30}$$

which yields the standard logarithmic expression for $\Delta T(r) = 2GM/(c^2 r)$ and a grazing path; precision tests include the Cassini radio experiment[8,9].

5.3. Light Deflection (Small Angle)

Let $\hat{\mathbf{t}}$ be the unit tangent to the ray. The Euler–Lagrange equation for (28) yields the isotropic ray equation

$$\frac{d}{ds}(n\,\hat{\mathbf{t}}) = \nabla n(\mathbf{x}). \tag{31}$$

Projecting perpendicular to the unperturbed direction and integrating along the path gives the net deflection

$$\hat{\alpha} \approx \int_{-\infty}^{+\infty} \nabla_\perp \ln n\,ds \approx \frac{1}{2}\int \nabla_\perp \Delta T\,ds, \tag{32}$$

to first order in ΔT. For a point mass,

$$\hat{\alpha} = \frac{4GM}{c^2\,b}, \tag{33}$$

the classic solar-limb value $1.75''$ when $b = R_\odot$[1,4,10]. The lensing geometry and small-angle deflection are illustrated in Figure 5.

5.4. Remarks on Validity and Coordinates

- Equations (30)–(33) assume a quasistatic, weak field and small deflection. For strong lensing or near horizons one should use the full $N^2 = 1 - \Delta T$ with the appropriate spatial metric; results coincide with GR in the bridge limit[1].
- The optical construction is coordinate-clean: ds is the physical arclength on the slice and $n(\mathbf{x})$ is a scalar built from $\Delta T(\mathbf{x})$.
- TD keeps cause/effect explicit: sources $\to \Delta T$ via the Poisson law; $\Delta T \to n$ sets all optical propagation.

[1] One can also view (29) as the statement that phases counted per unit *proper* time are invariant, while coordinate time dilates by $1/N$. The index n governs *propagation* below.

 doi:10.20944/preprints202511.2314.v1

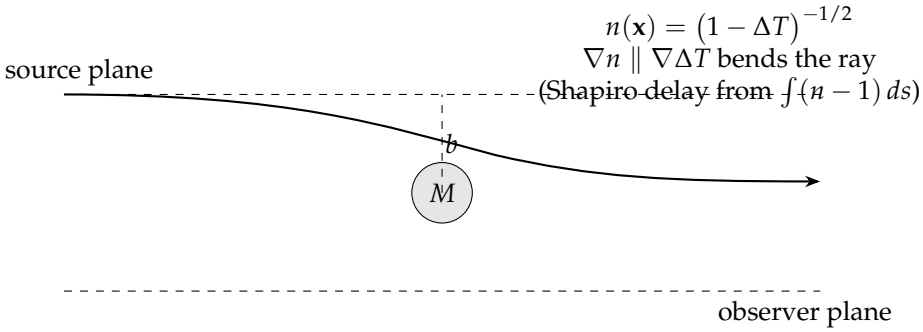

Figure 5. Lensing geometry in the index-of-time medium. Gradients of $n(\mathbf{x})$ (set by ΔT) deflect light by $\hat{\alpha}$ and produce the Shapiro delay; both recover the standard GR values in the weak field.

6. Horizons and the Mass–Size Law

In TD, horizons appear when the local slow–time share saturates the causal budget. This section defines the *black boundary* via $\Delta T = 1$, connects it to observable signatures, and states the linear mass–size calibration used as a global anchor for the framework.

6.1. Black Boundary: $\Delta T \to 1$ (lapse $N \to 0$)

For static observers $d\tau = N\, dt$ with $N^2 = 1 - \Delta T$ (Eq. (8)). The surface

$$\Delta T(\mathbf{x}) = 1 \qquad \Longleftrightarrow \qquad N(\mathbf{x}) = 0 \tag{34}$$

is a *black boundary*: a static worldline cannot be extended across it and the redshift from just outside to far away diverges[2,3]. In the TD optical picture the effective index $n = 1/\sqrt{1 - \Delta T}$ (Eq. (12)) diverges there, so the coordinate travel time blows up (Shapiro delay $\to \infty$) for paths that attempt to linger on the boundary. The profiles and the linear mass–size law are shown in Figure 6.

6.2. Spherically Symmetric Exterior and Monotonicity

For a compact, nonrotating, uncharged source, the weak–field identification

$$\Delta T(r) \;\approx\; \frac{2\,GM}{c^2\, r}, \qquad r \text{ outside the matter}, \tag{35}$$

increases monotonically inward. Its radial derivative, $\partial_r \Delta T = -2GM/(c^2 r^2) < 0$ (with r increasing outward), guarantees that ΔT grows toward the center. With $\Delta T \to 0$ at infinity and positive ρ_{active} (Eq. (11)), one has $0 \le \Delta T < 1$ in the exterior, approaching 1 only at a horizon[1,22].

6.3. Mass–Size Calibration (Nonrotating Case)

Matching the TD boundary $\Delta T = 1$ to the Schwarzschild event horizon fixes the linear mass–size law used throughout TD:

$$D_{\text{BH}} \;=\; 2\, r_s \;=\; \frac{4G}{c^2}\, M \;\equiv\; k\, M, \qquad k = \frac{4G}{c^2}. \tag{36}$$

Equation (36) is identical to Eq. (13) and serves as a *single global calibration* linking the slow–time normalization to the observed mass scale of black boundaries[2,3]. Observationally, horizon–scale imaging (e.g. M87*) is consistent with the GR horizon scale used here[25].

Remarks.

- The law (36) is stated for spherically symmetric, nonrotating, uncharged objects. Rotation or charge modify horizon locations (additional parameters enter); the calibration remains fixed by the Schwarzschild limit[2,3].

 doi:10.20944/preprints202511.2314.v1

- The *Normalization Axiom* $S \equiv c$ (Eq. (16)) is required to keep (36) and the weak–field identifications consistent with Newton/PPN[1].

6.4. Operational Signatures of Approaching a Black Boundary

Let A be far away ($\Delta T_A \simeq 0$) and B approach the boundary along a static worldline. Then

$$\frac{\nu_B}{\nu_A} = \sqrt{1 - \Delta T_B} \longrightarrow 0, \tag{37}$$

$$\Delta t_{\text{Shapiro}} = \frac{1}{2c} \int_\Gamma \Delta T \, ds \longrightarrow \infty, \tag{38}$$

$$n(\mathbf{x}) = \frac{1}{\sqrt{1 - \Delta T(\mathbf{x})}} \longrightarrow \infty. \tag{39}$$

Equations (37)–(39) summarize the TD optics/clock behavior: infinite redshift to infinity, divergent coordinate delay, and an unbounded index at the surface $\Delta T = 1$.

6.5. Pre–Clock Boundary vs. Black Boundary

It is important not to conflate:

Pre–clock: $S = 0$ (no baseline production of adjacency) *before* the universe begins; neither t, $d\tau$, nor ΔT are operationally defined.

Black boundary: $\Delta T \to 1$ with $S \equiv c$ already in place; static clocks stall locally ($N \to 0$), but the baseline runs elsewhere.

Only the latter appears in astrophysical settings.

6.6. Cosmological (de Sitter–Type) Horizon from Clock Drift

A uniform baseline drift $S(t) = c(1 + \varepsilon t + \cdots)$ (with small, nearly constant ε) induces an effective cosmological term $\Lambda = 3\varepsilon^2/c^2$ (Eq. (2)). The associated *cosmological horizon* has radius

$$r_{\text{dS}} = \frac{c}{\varepsilon} = \sqrt{\frac{3}{\Lambda}}, \tag{40}$$

distinct in origin from the local black boundary of Eq. (34). The former is a global feature of an expanding baseline; the latter is a local ΔT saturation near compact mass. The turnaround/balance scale $r_* = (GM/\varepsilon^2)^{1/3}$ introduced later (cosmology section) marks where the DE push equals the local slow–time gradient pull.

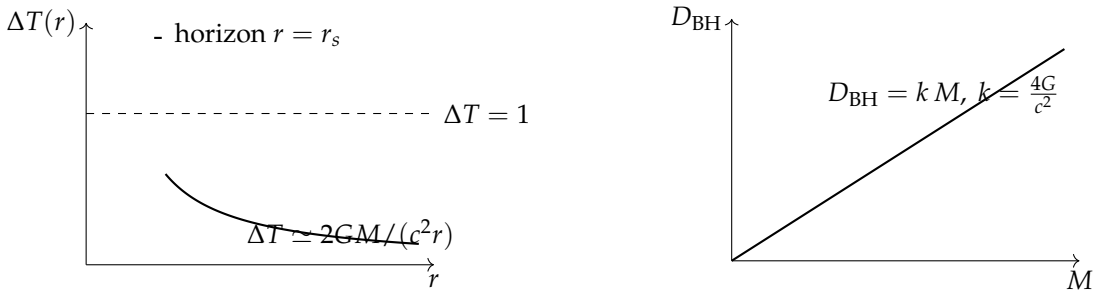

Figure 6. Horizons and the mass–size calibration. *Left:* Radial slow–time profile $\Delta T(r)$ approaches 1 at the black boundary ($N \to 0$). *Right:* Linear mass–size law $D_{\text{BH}} = 4GM/c^2$ used as the global calibration; consistent with the Schwarzschild limit and horizon–scale imaging[2,3,25].

7. Stress–Energy, Pressures, and Back–Reaction

Mass–energy does two things in TD: it *propagates* through a given slow–time landscape (via the index $n(\Delta T)$) and it *sources* the slow–time field ΔT that shapes that landscape. This section formalizes

 doi:10.20944/preprints202511.2314.v1

the sourcing side, including the role of pressures, and gives practical magnitudes from laboratory to astrophysical settings.

7.1. Active Density and the TD Source Law

In the weak, static regime TD uses the Poisson–type source law (Eq. (11))

$$\nabla^2 \Delta T \;=\; \frac{8\pi G}{c^2}\left(\rho + \frac{p_x + p_y + p_z}{c^2}\right) \;\equiv\; \frac{8\pi G}{c^2}\,\rho_{\text{active}}, \tag{41}$$

where ρ is energy density and p_i are principal pressures. For an *isotropic* fluid ($p_x = p_y = p_z = p$),

$$\rho_{\text{active}} \;=\; \rho + \frac{3p}{c^2}. \tag{42}$$

Special cases used repeatedly:

$$\text{Cold matter (dust)}: \quad p \approx 0 \;\Rightarrow\; \rho_{\text{active}} \approx \rho, \tag{43}$$

$$\text{Radiation / photon gas}: \quad p = \tfrac{1}{3}\rho c^2 \;\Rightarrow\; \rho_{\text{active}} = 2\rho. \tag{44}$$

Equations (41)–(44) mirror the standard weak–field GR result that *pressures gravitate* in addition to energy density[1,22]. The active-density cases used repeatedly are summarized in Table 4.

7.2. Electromagnetic Fields as Sources

Electromagnetic fields contribute through their energy and stresses. With

$$u_{\text{EM}} = \tfrac{1}{2}\left(\varepsilon_0 E^2 + \frac{B^2}{\mu_0}\right), \qquad \rho_{\text{EM}} = \frac{u_{\text{EM}}}{c^2}, \tag{45}$$

the Maxwell stress tensor implies $p_x + p_y + p_z = \rho_{\text{EM}} c^2$ (tracefree EM tensor), hence $\rho_{\text{active,EM}} = 2\rho_{\text{EM}}$ even for anisotropic static fields[26]. Free, isotropic radiation is the familiar case with $p = u_{\text{EM}}/3$ and the same factor of 2 via Eq. (44).

Propagation vs. sourcing (separation of roles).

Propagation: light follows Fermat in the effective index $n = 1/\sqrt{1 - \Delta T}$ (Eq. (12)); this is how EM *feels* a given ΔT (Sec. 5).
Sourcing: EM energy and stresses enter Eq. (41); this is how EM *creates* a (tiny) part of ΔT.

Table 4. Active density ρ_{active} for common sources (weak, static TD; cf. Eq. (42)). EM fields are tracefree so $p_x + p_y + p_z = \rho c^2$ even when anisotropic. A cosmological constant (vacuum energy) is not part of the local static Poisson problem but is shown for intuition; it gives negative active density and appears in TD as clock drift (Sec. 11).

Source	EoS / stresses	ρ_{active}
Cold matter (dust)	$p \approx 0$	ρ
Radiation / photon gas	$p = \rho c^2/3$	2ρ
Stiff fluid	$p = \rho c^2$	4ρ
Electromagnetic field (static)	tracefree T: $p_x + p_y + p_z = \rho c^2$	2ρ
Vacuum energy (Λ)	$p = -\rho c^2$	-2ρ

7.3. Why Rest Mass Usually "Slows Time More" in Practice

Per unit *energy density*, free radiation sources as strongly as (indeed twice as much as) cold matter [Eq. (44) vs. Eq. (43)]. In real systems, however, rest mass typically produces *steeper local gradients* because:

 doi:10.20944/preprints202511.2314.v1

1. **Localization/compactness:** rest mass can be packed and held in small R, creating large $|\nabla\Delta T| \sim \mathcal{O}(GM/(c^2R^2))$. Free radiation streams at c unless confined.
2. **Persistence:** rest mass sources are steady in their rest frame; transient radiation passes quickly, making its contribution fleeting at a given point.
3. **Confinement bookkeeping:** radiation in a box has pressure balanced by negative stresses of the walls; the net *active mass* of the isolated system is $E_{\rm tot}/c^2$. Boxes cannot be made arbitrarily compact without collapse, limiting achievable compactness relative to dense matter.

7.4. Practical Magnitudes

Laboratory field (1 T magnet).

Using $u_{\rm EM} \approx B^2/(2\mu_0)$,

$$u_{\rm EM} \sim 4 \times 10^5\,\mathrm{J\,m^{-3}}, \qquad \rho_{\rm EM} \sim 4 \times 10^{-12}\,\mathrm{kg\,m^{-3}}.$$

The resulting ΔT and its gradients are utterly negligible on laboratory scales (far below current clock sensitivities), though the concept is important.

High–intensity laser focus (illustrative).

With intensity I, the energy density is $u \approx I/c$. Even for $I \sim 10^{18}\,\mathrm{W\,m^{-2}}$,

$$u \sim 3 \times 10^9\,\mathrm{J\,m^{-3}}, \qquad \rho \sim 3 \times 10^{-8}\,\mathrm{kg\,m^{-3}},$$

still tiny gravitationally over micron–millimeter focal volumes.

Magnetar–scale field.

For $B \sim 10^{10}\,\mathrm{T}$,

$$u_{\rm EM} \sim 4 \times 10^{25}\,\mathrm{J\,m^{-3}}, \quad \rho_{\rm EM} \sim 4 \times 10^{8}\,\mathrm{kg\,m^{-3}}.$$

Over a region of size $L \sim 10\,\mathrm{km}$, the EM contribution alone would yield a surface–scale slow–time fraction of order

$$\Delta T_{\rm EM} \sim \frac{2\,G\,M_{\rm EM}}{c^2\,L} \sim \frac{2G}{c^2 L}\,\rho_{\rm EM}\,\frac{4\pi L^3}{3} \;\sim\; \text{a few} \times 10^{-10},$$

small compared to the star's baryonic gravity but no longer negligible as a correction in principle.

7.5. Back–Reaction Remains Linear at Small ΔT

Equations (41)–(42) are first order in ΔT (and time independent). This suffices for all weak, static applications in Secs. 4–6. Nonlinear or dynamical corrections can be organized as $\mathcal{O}(\Delta T^2)$ and $\mathcal{O}(\partial_t \Delta T)$ without changing the calibrations introduced earlier; we do not require them in this paper.

7.6. Equivalence Principle and Local Lorentz Invariance

TD respects local Lorentz invariance in the bridge regime ($S \equiv c$) and, in the weak field, couples test bodies universally through $\nabla\Delta T$ via Eq. (10). The "active density" that sources ΔT is the same combination that appears in weak–field GR[1,22]. No composition–dependent forces arise beyond standard tidal effects contained in $\nabla\nabla\Delta T$.

7.7. Summary (Sourcing vs. Propagation)

- **Sourcing:** mass–energy (including pressure) creates slow time via Eq. (41); the size of $|\nabla\Delta T|$ near a source is controlled primarily by compactness M/R^2 and persistence.
- **Propagation:** light and fields traverse a given ΔT landscape with effective index $n(\Delta T)$, producing redshift, delay, and bending as in Sec. 5.

 doi:10.20944/preprints202511.2314.v1

- **Practicality:** EM back–reaction is negligible in labs but conceptually essential; in extreme astrophysics it can be a small, principled correction to the dominant baryonic/degenerate matter sourcing.

8. Relation to GR (Bridge Pointer)

This section states—without re-deriving—how TD reproduces the tested content of GR when the baseline is frozen and variables are repackaged. Full algebra and degree-of-freedom (DoF) counting are provided in a separate bridge note[13].

8.1. Dictionary (Frozen Baseline)

Set the baseline to its calibrated value (Normalization Axiom, Eq. (16)):

$$S \equiv c, \tag{46}$$

and identify the ADM lapse with the slow–time field via

$$N^2 \;=\; 1 - \Delta T. \tag{47}$$

The spatial metric γ_{ij} and the shift N^i are unchanged (standard 3+1 split[6,7]). With Eq. (47), the TD optical and kinematic relations (Secs. 4–6) coincide with the standard GR weak–field formulas (Newtonian limit, gravitational redshift, Shapiro delay, light deflection)[1,4,8].

8.2. Action–Level Sketch and Constraints

In 3+1 form, the Einstein–Hilbert action reads[6,7]

$$S_{\rm EH} \;=\; \frac{c^3}{16\pi G}\int dt\, d^3x\, N\sqrt{\gamma}\left(R^{(3)} + K_{ij}K^{ij} - K^2\right), \tag{48}$$

where $\gamma \equiv \det\gamma_{ij}$, $R^{(3)}$ is the Ricci scalar of γ_{ij}, and K_{ij} is the extrinsic curvature. Substituting $N(\Delta T) = \sqrt{1-\Delta T}$ and varying gives, schematically,

$$\frac{\delta S_{\rm EH}}{\delta \Delta T} \;=\; \frac{\delta S_{\rm EH}}{\delta N}\,\frac{dN}{d\Delta T} \;=\; \frac{\delta S_{\rm EH}}{\delta N}\left(-\frac{1}{2N}\right), \tag{49}$$

so the lapse variation (Hamiltonian constraint) is reproduced up to the nonzero multiplicative factor $-1/(2N)$. The momentum constraint (variation of N^i) and the evolution equations (variation of γ_{ij}) are unchanged by the field redefinition. Thus the primary/secondary constraints and their algebra remain those of GR[6,7]; ΔT is a reparameterization of the lapse, not a new propagating field. A compact notation reference is given in Appendix H, Table H.

Constraints (for reference).

The Hamiltonian and momentum constraints keep their GR form,

$$\mathcal{H} \equiv R^{(3)} + K_{ij}K^{ij} - K^2 - \frac{16\pi G}{c^4}\,\mathcal{E} \;=\; 0, \tag{50}$$

$$\mathcal{H}_i \equiv -2\nabla_j\Big(K^j{}_i - \delta^j{}_i K\Big) - \frac{16\pi G}{c^4}\,\mathcal{P}_i \;=\; 0, \tag{51}$$

with matter energy density $\mathcal{E}$ and momentum density $\mathcal{P}_i$ measured by the N–normal observers (notation fixed here; derivation not repeated).

8.3. Degrees of Freedom and Gauge

Because N is nondynamical in GR (a Lagrange multiplier), the redefinition $N^2 = 1 - \Delta T$ does not introduce a new radiative DoF. Linearizing around Minkowski ($\Delta T = 0$, $N = 1$, $\gamma_{ij} = \delta_{ij}$, $N^i = 0$)

 doi:10.20944/preprints202511.2314.v1

yields the standard two *tensor* polarizations propagating at c; any lapse perturbation is gauge (non-propagating)[1,3]. Hence TD in the bridge regime has the same local Lorentz invariance and GW content as GR, consistent with observations[11,12].

8.4. PPN and Tested Weak–Field Phenomenology

With $S \equiv c$ and Eq. (47), the Parametrized Post-Newtonian (PPN) parameters in the weak field are

$$\gamma_{\mathrm{PPN}} = 1, \qquad \beta_{\mathrm{PPN}} = 1, \tag{52}$$

and the classic tests are reproduced:

- Newtonian limit from $\mathbf{g} = -(c^2/2)\nabla\Delta T$ with $\Delta T = 2GM/(c^2 r)$;
- gravitational redshift $\nu_B/\nu_A = \sqrt{(1-\Delta T_B)/(1-\Delta T_A)}$;
- Shapiro delay $\Delta t \approx (2GM/c^3)\ln(\cdots)$;
- light deflection $\hat{\alpha} = 4GM/(c^2 b)$,

in agreement with precision tests including Cassini[9] and classic eclipse measurements[10] (see also Secs. 4–5).

8.5. Rotating Solutions (Kerr) and the Lapse

For stationary, axisymmetric spacetimes the metric in 3+1 form involves (N, N^i, γ_{ij}). The bridge identifies

$$\Delta T \;=\; 1 - N^2_{(\text{Kerr slice})}, \tag{53}$$

where $N_{(\text{Kerr slice})}$ is the lapse of the chosen foliation (e.g., Boyer–Lindquist or horizon–penetrating slices). Since TD leaves γ_{ij} and N^i untouched, all Kerr observables (ISCO, lensing, redshift, frame dragging) are inherited from the GR solution in the same slice[2,3]. The surface $\Delta T \to 1$ matches the $N \to 0$ behavior at the horizon.

8.6. Gravitational Waves

Linearizing the bridge variables yields the standard transverse–traceless wave equation on Minkowski (and on weak backgrounds),

$$\Box\, h^{\mathrm{TT}}_{ij} \;=\; 0, \qquad \text{speed} \;= c, \tag{54}$$

with no additional scalar mode, consistent with GW speed bounds and polarization tests[11,12].

8.7. Scope and Limits of the Bridge

The mapping assumes (i) $S \equiv c$ (frozen baseline), and (ii) regions where $N > 0$ (outside horizons in the chosen slicing). Inside horizons a different foliation is required; TD treats that by construction via the $\Delta T \to 1$ boundary (Sec. 6). Cosmological applications that allow a tiny uniform drift $S(t) = c(1 + \varepsilon t + \cdots)$ fall outside the strict bridge (since $\dot{S} \neq 0$), but their homogeneous effect can be summarized by

$$\Lambda(t) \;=\; \frac{3\,\varepsilon(t)^2}{c^2}, \tag{55}$$

and treated observationally as GR+$\Lambda(t)$ (Sec. 11).

Pointer to companion note

A separate bridge note[13] provides: (i) the explicit substitution of Eq. (47) into Eq. (48); (ii) the chain–rule variation Eq. (49) and the unchanged constraint algebra; (iii) a linear PPN calculation confirming $\beta = \gamma = 1$; (iv) a Kerr checklist in Boyer–Lindquist and Kerr–Schild slices; and (v) the GW linearization showing only two tensor modes at speed c.

 doi:10.20944/preprints202511.2314.v1

9. Electromagnetism on a TD Background

Electromagnetism (EM) interacts with TD in two clean ways: (i) *propagation*—light and EM waves travel in a vacuum that behaves like a medium with index $n(\mathbf{x})$ set by the slow–time field ΔT; (ii) *sourcing*—EM energy and stresses contribute (weakly) to the field equation that determines ΔT. This section writes both pieces in a compact, operational form.

9.1. Maxwell on a Static TD Slice: Effective Medium

On a static slice with lapse N and spatial metric γ_{ij},

$$ds^2 \;=\; -N^2c^2\,dt^2 + \gamma_{ij}\,dx^i dx^j, \tag{56}$$

vacuum electrodynamics is equivalent to Maxwell in an *isotropic medium* with[1,4,27,28]

$$N^2 = 1-\Delta T, \qquad n(\mathbf{x}) \;=\; \frac{1}{N(\mathbf{x})} \;=\; \frac{1}{\sqrt{1-\Delta T(\mathbf{x})}}, \tag{57}$$

and relative parameters $\varepsilon_r(\mathbf{x}) = \mu_r(\mathbf{x}) = n(\mathbf{x})$ (so the vacuum *impedance* remains $Z_0 = \sqrt{\mu_0/\varepsilon_0}$). Writing $\mathbf{D} = \varepsilon_0 n\,\mathbf{E}$, $\mathbf{B} = \mu_0 n\,\mathbf{H}$, the macroscopic Maxwell system becomes

$$\nabla\cdot(n\,\mathbf{E}) = \frac{\rho_f}{\varepsilon_0}, \tag{58}$$

$$\nabla\times\mathbf{H} - \frac{\partial}{\partial t}(\varepsilon_0 n\,\mathbf{E}) = \mathbf{J}_f, \tag{59}$$

$$\nabla\cdot\mathbf{B} = 0, \qquad \nabla\times\mathbf{E} + \frac{\partial\mathbf{B}}{\partial t} = 0. \tag{60}$$

When $n = n(\mathbf{x})$ varies slowly in time (quasistatic TD) the modification is the spatial dependence in Eqs. (58)–(59); the *local* light speed measured by comoving observers remains c, while the *coordinate* phase/group speeds are c/n.

9.2. Wave, Ray, and Redshift Relations

In the geometric–optics limit (slowly varying n), the eikonal S obeys $|\nabla S| = \frac{\omega}{c}\,n(\mathbf{x})$, and the travel time functional is Fermat's

$$T[\Gamma] \;=\; \frac{1}{c}\int_\Gamma n(\mathbf{x})\,ds, \tag{61}$$

so rays satisfy $d(n\hat{\mathbf{t}})/ds = \nabla n$ and bend toward larger n (larger ΔT), reproducing Eqs. (30)–(33). For scalar envelopes (ignoring polarization) one may use the Helmholtz form

$$\nabla^2\Psi + \frac{\omega^2}{c^2}\,n^2(\mathbf{x})\,\Psi \;\approx\; 0 \qquad (\text{GO / weak gradients } \nabla n), \tag{62}$$

with amplitude transport corrections when ∇n is not negligible.

Clock comparisons are set by the lapse (not by n): for static observers

$$\frac{\nu_B}{\nu_A} = \frac{N_B}{N_A} = \sqrt{\frac{1-\Delta T_B}{1-\Delta T_A}} \;\approx\; 1 - \tfrac{1}{2}(\Delta T_B - \Delta T_A), \tag{63}$$

as in Eq. (29). Thus TD cleanly separates *propagation* (via n) from *rate* (via N).

9.3. Sourcing of ΔT by EM

EM fields gravitate through their energy density and stresses. With

$$u_{\mathrm{EM}} = \tfrac{1}{2}\left(\varepsilon_0 E^2 + \frac{B^2}{\mu_0}\right), \qquad \rho_{\mathrm{EM}} = \frac{u_{\mathrm{EM}}}{c^2}, \tag{64}$$

 doi:10.20944/preprints202511.2314.v1

the weak, static TD source law (Eq. (41)) gives

$$\nabla^2 \Delta T \;=\; \frac{8\pi G}{c^2}\left(\rho + \frac{p_x + p_y + p_z}{c^2}\right), \tag{65}$$

so free, isotropic radiation ($p = \rho c^2/3$) contributes $\rho_{\text{active}} = 2\rho$, and more generally trace–free EM stresses imply $p_x + p_y + p_z = \rho c^2 \Rightarrow \rho_{\text{active}} = 2\rho$[26]. In laboratories this back–reaction is negligible; in extreme astrophysics (magnetars, pair fireballs) it can be a principled correction.

9.4. Two Compact Observables

Cavity frequency shift (local test).

For a rigid cavity of proper length L at position $\mathbf{x}$, the mth longitudinal mode obeys

$$\omega_m(\mathbf{x}) \;\approx\; \frac{m\pi c}{n(\mathbf{x})\, L} \;\Rightarrow\; \frac{\delta\omega}{\omega} \;\approx\; -\frac{\delta n}{n} \;\approx\; -\frac{1}{2}\,\delta\Delta T, \tag{66}$$

consistent with the gravitational redshift: moving the cavity upward by Δh on Earth gives $\delta\omega/\omega \approx +g\,\Delta h/c^2$ (since ΔT decreases with altitude)[19]. The setup is sketched in Figure 7.

Fiber/space link Shapiro test (field test).

For a phase link Γ past a compact body,

$$\Delta t_{\text{Shapiro}} \;\approx\; \frac{1}{2c}\int_\Gamma \Delta T\, ds, \tag{67}$$

matching the standard $\sim (2GM/c^3)\ln(\cdots)$ result for a solar graze[8,9].

9.5. Additivity with Ordinary Media (Index Bookkeeping)

If light also traverses a material medium with refractive index n_{mat}, then to first order in ΔT

$$n_{\text{eff}} \;=\; n_{\text{mat}}\, n(\Delta T) \;\approx\; n_{\text{mat}}\left(1 + \tfrac{1}{2}\Delta T\right), \tag{68}$$

so gravitational and material contributions factor multiplicatively (additively in $\ln n$). This is useful for metrology setups (fibers, cells) where one separates material dispersion from TD contributions.

9.6. Gauge and Charge Conservation

Equations (58)–(60) preserve charge conservation exactly:

$$\frac{\partial \rho_f}{\partial t} + \nabla\cdot\mathbf{J}_f \;=\; 0, \tag{69}$$

since $n(\mathbf{x})$ is time–independent in the quasistatic TD approximation. Gauge freedom of the four–potential is unchanged; TD does not alter EM gauge symmetry.

9.7. Scope and Limits

The medium picture (57) assumes (i) a static or slowly varying TD background ($\partial_t \Delta T \approx 0$ during measurement), and (ii) weak fields ($\Delta T \ll 1$) for the isotropic index. Near horizons or in strongly curved regions one should use the full $N^2 = 1 - \Delta T$ with the appropriate γ_{ij} (the bridge reproduces the GR geometric–optics limit exactly).

 doi:10.20944/preprints202511.2314.v1

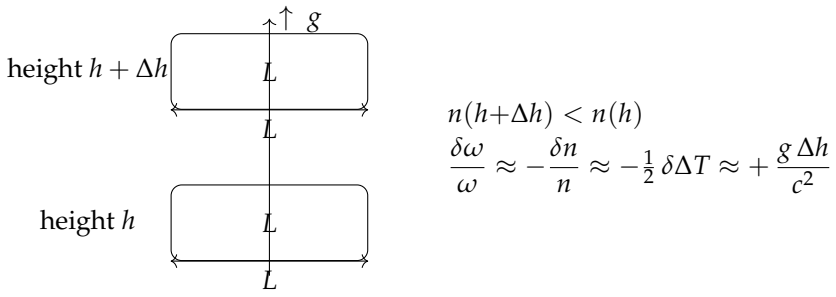

Figure 7. Cavity redshift as an index effect. Raising a rigid cavity by Δh changes $n(\mathbf{x}) = (1 - \Delta T)^{-1/2}$ and shifts the mode frequency according to Eq. (66), consistent with the gravitational redshift.

10. Quantum–Ready Observables (No New Degrees of Freedom)

In this section we treat $\Delta T(\mathbf{x})$ as a *classical* background (bridge regime with $S \equiv c$) and quantize matter/EM fields on top of it, exactly as in QFT on curved spacetime. Quantum phases accrue from *proper time* $d\tau = N\, dt$ with $N^2 = 1 - \Delta T$ (Eq. (8)); this yields immediate, testable predictions for clocks, interferometers, and cavities without introducing a new propagating gravitational mode.

10.1. Universal Phase from Proper Time

For any stationary energy eigenstate with local energy E, the quantum phase along a worldline is

$$\phi \;=\; -\frac{1}{\hbar}\int E\, d\tau \;=\; -\frac{1}{\hbar}\int E\, N\, dt \;\approx\; -\frac{1}{\hbar}\int E\Big(1 - \tfrac{1}{2}\Delta T\Big)\, dt, \tag{70}$$

so the *TD contribution* to the differential phase between two paths A, B is

$$\Delta\phi_{\mathrm{TD}} \;\equiv\; \phi_B - \phi_A \;\approx\; -\frac{1}{2\hbar}\int_{t_i}^{t_f} \big[E_B\, \Delta T_B - E_A\, \Delta T_A\big]\, dt. \tag{71}$$

In the nonrelativistic limit, taking $E \simeq mc^2$ and $\Delta T \simeq 2\Phi/c^2$ with Newtonian potential Φ reproduces the standard gravitational phases[1].

10.2. Atom Interferometers (Mach–Zehnder Class)

Consider two branches separated vertically in a uniform field (approximately constant $\nabla\Delta T$). Using Eq. (71) with $E \simeq mc^2$ and $\Delta T \simeq 2\Phi/c^2 \simeq 2gz/c^2$,

$$\Delta\phi_{\mathrm{TD}} \;\approx\; -\frac{m}{\hbar}\int (\Phi_B - \Phi_A)\, dt \;\to\; k_{\mathrm{eff}}\, g\, T^2, \tag{72}$$

the usual Kasevich–Chu result (k_{eff} two-photon momentum transfer; T pulse separation)[29,30]. Thus TD predicts the *same* inertial response as GR/Newton in the bridge regime; the equivalence principle holds at this order. Our Mach–Zehnder geometry is shown in Figure 8.

10.3. Quantum Clocks (Ramsey and Comparisons)

Two identical clocks at A, B with transition energy $\Delta E = \hbar\omega_0$ accumulate a Ramsey phase difference

$$\Delta\phi_{\mathrm{clock}} \;=\; -\frac{\Delta E}{\hbar}\int (d\tau_B - d\tau_A) \;=\; -\omega_0 \int \big(N_B - N_A\big)\, dt \;\approx\; \frac{\omega_0}{2}\int (\Delta T_B - \Delta T_A)\, dt, \tag{73}$$

consistent with the redshift relation $\nu_B/\nu_A = \sqrt{(1 - \Delta T_B)/(1 - \Delta T_A)}$ (Eqs. (18), (29)). For a vertical separation Δh on Earth and interrogation time T_{int},

$$\frac{\Delta\nu}{\nu} \;\approx\; \frac{g\,\Delta h}{c^2}, \qquad \Delta\phi_{\mathrm{clock}} \;\approx\; \omega_0\, \frac{g\,\Delta h}{c^2}\, T_{\mathrm{int}}, \tag{74}$$

 doi:10.20944/preprints202511.2314.v1

as observed with modern optical clocks[19–21].

10.4. Optical Cavities and Photons

For a rigid cavity of proper length L at location $\mathbf{x}$, the longitudinal resonance is

$$\omega_m(\mathbf{x}) \approx \frac{m\pi c}{n(\mathbf{x})\,L}, \qquad n(\mathbf{x}) = \frac{1}{\sqrt{1-\Delta T(\mathbf{x})}}, \tag{75}$$

so a small change $\delta\Delta T$ produces

$$\frac{\delta\omega}{\omega} \approx -\frac{1}{2}\,\delta\Delta T, \tag{76}$$

as stated in Sec. 9. Raising the cavity by Δh gives $\delta\omega/\omega \approx +g\,\Delta h/c^2$ (since ΔT decreases with altitude)[19].

10.5. Matter–Wave Gravimetry from $\nabla\Delta T$

Using the operational gradient relation (Eq. (21)),

$$\mathbf{g}(\mathbf{x}) = -\frac{c^2}{2}\,\nabla\Delta T(\mathbf{x}), \tag{77}$$

any instrument that measures $\Delta\phi$ along two nearby paths can be recast as a sensor of $\nabla\Delta T$. In atom interferometers the standard sensitivity is

$$\delta g \simeq \frac{\delta\phi}{k_{\text{eff}}\,T^2}, \tag{78}$$

so mapping $\nabla\Delta T$ is equivalent to gravimetry at the quoted precision[30].

10.6. Optional: Stochastic Slow–Time Noise (Bounds Only)

If one phenomenologically allows tiny, stationary fluctuations $\delta\Delta T(t)$ around the static background (still no new propagating DoF), the phase in Eq. (70) becomes stochastic. Defining the one-sided PSD $S_{\Delta T}(\omega)$ and a temporal weighting window $w(t)$ (interferometer or Ramsey sequence),

$$\sigma_\phi^2 \approx \left(\frac{E}{2\hbar}\right)^2 \int_0^\infty S_{\Delta T}(\omega)\,|\tilde{w}(\omega)|^2\,d\omega, \tag{79}$$

with $\tilde{w}$ the Fourier transform of w. Observed contrasts then bound $S_{\Delta T}(\omega)$. This is an *optional* TD phenomenology; in the main text we set $\delta\Delta T = 0$.

10.7. Gauge, Locality, and Consistency

- **Local Lorentz:** In the bridge regime ($S \equiv c$) local Lorentz invariance holds; N rescales coordinate time but does not alter local light cones.
- **Gauge independence:** Eqs. (70)–(73) depend only on proper times and on ΔT differences measured by clocks; no coordinate choice enters.
- **No extra graviton:** We do not add a scalar gravitational wave; ΔT is a reparameterization of the lapse. Quantum tests here probe the *background* slow–time field, not a new radiation channel[1].

 doi:10.20944/preprints202511.2314.v1

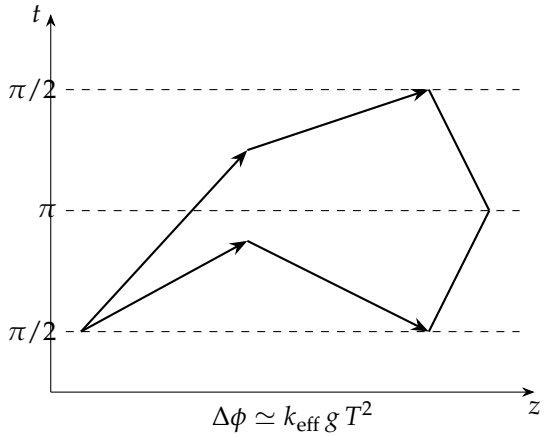

Figure 8. Mach–Zehnder atom interferometer in a uniform field. The TD background enters phases via $d\tau = N\,dt$ and $\Delta T \simeq 2gz/c^2$, yielding the standard $k_{\rm eff} g T^2$ signal (Eq. (72)).

10.8. Takeaway

TD turns quantum sensors into direct probes of the slow–time field: phases scale with integrals of ΔT (or its gradients), while spectra and contrasts can, in principle, bound any tiny stochastic component of ΔT. In the frozen baseline, all predictions reduce to those of GR in the tested regimes; the framework is thus ready for near–term quantum tests without additional assumptions. Key quantum observables and their leading TD dependences are collected in Table 5.

Table 5. Quantum-ready observables and their leading TD dependences in the bridge regime ($S \equiv c$) and weak, quasistatic fields ($\Delta T \ll 1$). Phases come from proper time $d\tau = N\,dt$ with $N^2 = 1 - \Delta T$; the Shapiro entry reduces to the standard GR expression [8].

Observable	Leading TD dependence
Atom interferometer phase	$\Delta\phi \approx -\frac{m}{\hbar}\int(\Phi_B - \Phi_A)\,dt \;\leftrightarrow\; k_{\rm eff} g T^2$
Clock comparison (Ramsey)	$\frac{\Delta\nu}{\nu} \approx \frac{1}{2}(\Delta T_B - \Delta T_A) \approx \frac{g\,\Delta h}{c^2}$
Cavity frequency shift	$\frac{\delta\omega}{\omega} \approx -\frac{1}{2}\,\delta\Delta T$
Photon time transfer (Shapiro)	$\Delta t \approx \frac{1}{2c}\int \Delta T\,ds$

11. Cosmology in TD

In homogeneous cosmology the TD baseline may drift slowly in time,

$$S(t) = c\,[1 + \delta s(t)], \qquad \varepsilon(t) \;\equiv\; \frac{\dot S(t)}{c} \;=\; \dot{\delta s}(t), \tag{80}$$

with ε small and (on Hubble times) nearly constant. In the *pure baseline* limit (no matter/radiation), TD gives de–Sitter–like expansion

$$H(t) \;=\; \frac{\dot a}{a} \;=\; \varepsilon(t), \qquad a(t) \;\propto\; \exp\!\Big(\int \varepsilon\,dt\Big). \tag{81}$$

More generally, when matter and radiation are present and the baseline drift is uniform in space, TD is observationally equivalent to GR with a (possibly mild) time–dependent cosmological term

$$\boxed{\Lambda(t) \;=\; \frac{3\,\varepsilon(t)^2}{c^2}} \quad\Longrightarrow\quad H^2 \;=\; \frac{8\pi G}{3}\rho \;-\; \frac{kc^2}{a^2} \;+\; \frac{\Lambda(t)\,c^2}{3}. \tag{82}$$

 doi:10.20944/preprints202511.2314.v1

11.1. A Minimal One–Parameter Extension

To test for tiny departures from ΛCDM, adopt

$$\varepsilon(z) \;=\; \varepsilon_0\,(1+z)^p, \qquad |p| \ll 1, \tag{83}$$

so that

$$\Lambda(z) \;=\; \Lambda_0\,(1+z)^{2p}, \qquad \Lambda_0 \equiv \frac{3\,\varepsilon_0^2}{c^2}. \tag{84}$$

Define the present–day density parameters $\Omega_{m0},\ \Omega_{r0},\ \Omega_{k0},\ \Omega_{\Lambda 0} \equiv \varepsilon_0^2/H_0^2$ (so $\Omega_{m0}+\Omega_{r0}+\Omega_{k0}+\Omega_{\Lambda 0}=1$). Then

$$\boxed{E^2(z) \;\equiv\; \frac{H^2(z)}{H_0^2} \;=\; \Omega_{m0}(1+z)^3 + \Omega_{r0}(1+z)^4 + \Omega_{k0}(1+z)^2 + \Omega_{\Lambda 0}\,(1+z)^{2p}}, \tag{85}$$

which reduces to ΛCDM when $p=0$.

11.2. Distances and Horizons

Standard distance measures follow[31]:

$$\chi(z) = \int_0^z \frac{c\,dz'}{H(z')}, \tag{86}$$

$$D_M(z) = \begin{cases} \chi, & \Omega_{k0}=0, \\ \frac{c}{H_0\sqrt{\Omega_{k0}}}\,\sinh\!\Big(\sqrt{\Omega_{k0}}\,\frac{H_0\chi}{c}\Big), & \Omega_{k0}>0, \\ \frac{c}{H_0\sqrt{-\Omega_{k0}}}\,\sin\!\Big(\sqrt{-\Omega_{k0}}\,\frac{H_0\chi}{c}\Big), & \Omega_{k0}<0, \end{cases} \tag{87}$$

$$D_L(z) = (1+z)\,D_M(z), \qquad D_A(z) = \frac{D_M(z)}{1+z}. \tag{88}$$

A uniform baseline drift also implies a *cosmological (de–Sitter) horizon*

$$r_{\rm dS}(t) \;=\; \frac{c}{\varepsilon(t)} \;=\; \sqrt{\frac{3}{\Lambda(t)}}, \tag{89}$$

distinct from local black boundaries ($\Delta T \to 1$). A visual summary of the TD cosmology pieces appears in Figure 9.

11.3. Bound vs. Unbound: the TD Turnaround Scale

Balancing the inward slow–time gradient pull against the outward baseline push gives the TD turnaround radius

$$\boxed{r_*(M,t) \;=\; \Big(\frac{GM}{\varepsilon(t)^2}\Big)^{1/3} \;=\; \Big(\frac{3GM}{\Lambda(t)\,c^2}\Big)^{1/3}} \tag{90}$$

inside which structures can remain bound (quasi–static) and outside which the uniform drift dominates. This mirrors the ΛCDM turnaround scale[32] and provides a direct, falsifiable link from the clock drift to group/cluster environments.

11.4. Growth of Structure (Linear Regime)

Writing derivatives with respect to $\ln a$, the linear growth factor $D(a)$ satisfies

$$\frac{d^2D}{d(\ln a)^2} \;+\; \Big[2+\frac{d\ln H}{d\ln a}\Big]\frac{dD}{d\ln a} \;-\; \frac{3}{2}\,\Omega_m(a)\,D \;=\; 0, \tag{91}$$

 doi:10.20944/preprints202511.2314.v1

with $\Omega_m(a) = \frac{\Omega_{m0}a^{-3}}{E^2(a)}$ and $E(a)$ from Eq. (85) via $a = 1/(1+z)$[33]. In the TD extension the effective dark–energy term keeps $w(z) = -1$ (pressure $= -\rho c^2$) but its amplitude varies as $(1+z)^{2p}$; growth–index parameterizations $f = \Omega_m(a)^\gamma$ remain approximately valid with small shifts controlled by p through $d\ln H/d\ln a$[34].

11.5. Observational Program (Concise)

- **Distances:** Fit p using SN Ia $D_L(z)$, BAO (D_M/r_d, $H(z)\,r_d$), and cosmic chronometers $H(z)$ with Eq. (85)[14–16,35]. Report $p=0$ as ΛCDM and bounds as $|p| < \cdots$ (95%).
- **Growth:** Constrain p with redshift–space distortions $f\sigma_8(z)$ via Eq. (91); check consistency with distance fits[36].
- **Turnaround/radii:** Compare Eq. (90) with zero–velocity surfaces / splashback radii of groups and clusters (environment modeling required)[32].
- **Horizon scale:** Use Eq. (89) for intuition and consistency checks; it sets the limiting comoving scale for causal influence in a drift–dominated epoch.

11.6. Limits and Degeneracies

Small p is partially degenerate with (w_0, w_a) reparameterizations and with Ω_{k0}. Joint fits should either (i) fix curvature to a Planck–consistent prior and report p, or (ii) explore (p, Ω_{k0}) jointly and quote marginalized bounds[36]. By construction $p \to 0$ recovers ΛCDM exactly.

11.7. Genesis in TD (One Paragraph)

In TD the universe begins when the clock turns on ($S > 0$). An early phase with large, nearly constant ε smooths the universe (inflation–like), then ε decays and reheats into fields; later, a tiny residual ε_0 drives the present acceleration. This reframes the GR singularity as a *pre–clock* boundary ($S = 0$) rather than a curvature blow–up, and ties the entire expansion history to the single causal rate $\varepsilon(t)$.

Key equations (for quick reference)

$$\begin{aligned}
\Lambda(t) &= \frac{3\varepsilon(t)^2}{c^2},\\
E^2(z) &= \Omega_{m0}(1+z)^3 + \Omega_{r0}(1+z)^4 + \Omega_{k0}(1+z)^2 + \Omega_{\Lambda 0}(1+z)^{2p},\\
D_L(z) &= (1+z)D_M(z),\\
r_{\rm dS} &= c/\varepsilon,\\
r_*(M) &= (GM/\varepsilon^2)^{1/3}.
\end{aligned}$$

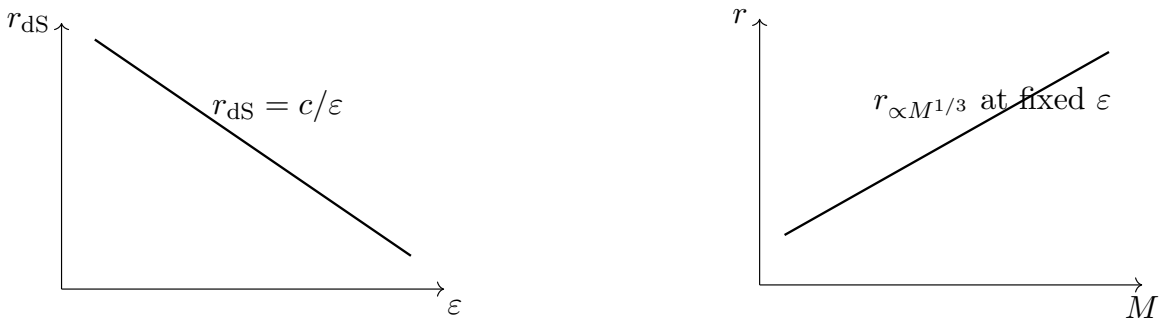

(a) de–Sitter horizon vs. drift (b) Turnaround radius scaling

Figure 9. Cosmology in TD: key scalings. (a) The horizon scale is set by the baseline drift, $r_{\rm dS} = c/\varepsilon$. (b) The TD turnaround radius scales as $r_* \propto M^{1/3}$ for fixed ε, matching the ΛCDM expression with $\Lambda = 3\varepsilon^2/c^2$.

 doi:10.20944/preprints202511.2314.v1

12. Experiments and Observational Program

This section turns the TD relations into concrete measurements; representative magnitudes are listed in Table 6. We split the program into (i) laboratory/near–Earth tests that probe ΔT and its gradient directly, (ii) astronomical tests of photon propagation, and (iii) cosmological fits that constrain a possible clock drift $\varepsilon(t)$.

12.1. Laboratory and Near–Earth (Direct ΔT Mapping)

Clock networks (primary).

Deploy identical or cross–calibrated clocks at $\{\mathbf{x}_i\}$; measure frequency ratios $\nu(\mathbf{x}_j)/\nu(\mathbf{x}_i)$ with two–way links. Using Eq. (21),

$$\mathbf{g}(\mathbf{x}) \;=\; -\frac{c^2}{2}\,\nabla\Delta T(\mathbf{x}) \;\approx\; c^2\,\nabla\ln\nu(\mathbf{x}). \tag{92}$$

A vertical pair separated by Δh gives, from Eq. (24),

$$\frac{\Delta\nu}{\nu} \;\approx\; \frac{g\,\Delta h}{c^2} \;\approx\; 1.1\times10^{-16}\times\Big(\frac{\Delta h}{1\ \mathrm{m}}\Big),$$

consistent with state–of–the–art optical clocks and satellite comparisons[19–21]. *Deliverable:* a 2D map of $\Delta T(\mathbf{x})$ (Dirichlet/Neumann reconstruction; Eq. (23)), and a direct test that $-\frac{c^2}{2}\nabla\Delta T$ matches local gravimetry.

Atom interferometers.

In a Mach–Zehnder geometry, the phase follows Eq. (72): $\Delta\phi \simeq k_{\mathrm{eff}} g T^2$. Operate the interferometer on multiple baselines to sample $\nabla\Delta T$ spatially; compare to classical gravimeters and the clock–inferred field[29,30].

Cavity frequency shifts.

A rigid cavity of proper length L moved by Δh satisfies Eq. (76): $\delta\omega/\omega \approx +g\,\Delta h/c^2$ (since ΔT decreases with altitude). *Use:* photon–based check of the clock result with different systematics[19].

Shapiro on fiber/microwave links.

Route a phase–stable link along a path Γ past known mass distributions; the additional delay is $\Delta t \approx \frac{1}{2c}\int_\Gamma \Delta T\,ds$ [Eq. (30)]. *Design:* pick routes with strong known potentials (mountain shoulders, urban towers); compare with predictions from ΔT reconstructed by the clock grid.

Source inversion (optional).

With a bounded domain Ω, solve Eq. (11) to estimate ρ_{active} from the reconstructed ΔT map. *Caveat:* boundary modeling and noise regularization dominate errors.

12.2. Astronomical Propagation Tests

Solar–system timing.

Radio/laser ranging with impact parameter $b \sim R_\odot$ yields the one–way Shapiro delay $\Delta t \sim (2GM_\odot/c^3)\ln(\cdots) \approx 120\ \mu$s (Sec. 4), consistent with Cassini tests[8,9]. This directly matches Eq. (30) with $\Delta T(r) = 2GM_\odot/(c^2 r)$.

Light deflection and time delays.

Weak deflection $\hat{\alpha} = 4GM/(c^2 b)$ [Eq. (33)] and strong–lens time delays follow from the Fermat functional $T[\Gamma] = c^{-1}\int n\,ds$ [Eq. (28)]. *Program:* rephrase lens models in ΔT to provide a uniform TD/GR dictionary for deflection and delays[4,10].

 doi:10.20944/preprints202511.2314.v1

12.3. Cosmology: Distances, Growth, and Key Scales

Distance ladder (primary).

Fit the one–parameter TD extension via $E^2(z)$ in Eq. (85). Use SNe Ia luminosity distances $D_L(z)$, BAO (D_M/r_d, $H(z)r_d$), and cosmic chronometers $H(z)$; report p (Eq. (83)) with uncertainties and the $p = 0$ (ΛCDM) limit[14–16,35,36].

Growth and RSD.

Use the linear growth equation Eq. (91) to predict $f\sigma_8(z)$ and compare with redshift–space distortion data; check distance/growth consistency[34,36].

Turnaround and splashback radii.

Compare the TD turnaround scale $r_*(M,t) = (GM/\varepsilon^2)^{1/3}$ [Eq. (90)] with observed zero–velocity or splashback radii of groups/clusters (environment modeling required)[32].

12.4. How to Report (Falsifiable Targets)

1. **Local gradient law:** publish $\Delta T(\mathbf{x})$ maps and verify $\mathbf{g}(\mathbf{x}) + \frac{c^2}{2}\nabla\Delta T(\mathbf{x}) = 0$ within errors over the domain. Any systematic, coordinate–independent violation falsifies TD (or the weak/quasistatic approximation).
2. **Optical dictionary:** for any measured delay/deflection, provide the corresponding line integral of ΔT (Eqs. (30), (32)) sourced by the same mass model; mismatches falsify the unified index picture.
3. **Cosmology:** report p with a clear prior on Ω_{k0}; if p is consistent with 0, give a 95% upper bound. Publish $r_*(M)$ comparisons with explicit environment systematics.

12.5. Systematics and Error Budgets (Checklist)

- **Clocks/links:** Allan deviation, transfer noise, temperature/strain of fibers, tidal loading, atmospheric delay (for free–space).
- **Gravimetry:** instrument tilt, vibration, Coriolis effects for atom interferometers; co–location with clocks for common–mode rejection.
- **Cavities:** thermoelastic and refractive changes in materials; local acceleration sensitivity (mount design).
- **Timing/propagation:** ephemerides, plasma dispersion, tropospheric delay; impact parameter uncertainties.
- **Cosmology:** calibration systematics in SN Ia; BAO reconstruction choices; chronometer stellar population modeling; RSD velocity bias; curvature degeneracy with p.

Table 6. Compact targets and typical magnitudes for near-term tests. Weak-field optical entries reduce to standard GR results for a point mass (Shapiro delay [8]; solar-limb deflection [4,10]).

Observable	Leading dependence	Typical scale
Clock redshift (1 m)	$\Delta\nu/\nu \approx g\,\Delta h/c^2$	1.1×10^{-16} per m
AI phase	$\Delta\phi \approx k_{\rm eff}\, g\, T^2$	e.g. $k_{\rm eff} \sim 10^7$ m^{-1}, $T \sim 0.1$ s
Cavity shift	$\delta\omega/\omega \approx -\frac{1}{2}\,\delta\Delta T$	same sign/magnitude as clock shift
Shapiro (solar graze)	$\Delta t \approx (2GM_\odot/c^3)\ln(\cdots)$	$\sim 120\,\mu$s (one–way)
Deflection (Sun limb)	$\hat{\alpha} = 4GM_\odot/(c^2R_\odot)$	$1.75''$
Turnaround scale	$r_* = (GM/\varepsilon^2)^{1/3}$	~ 1 Mpc for $10^{12}M_\odot$
dS horizon	$r_{\rm dS} = c/\varepsilon$	$\sim c/H_0$ today

12.6. Roadmap and Milestones

1. **Local:** produce a campus–scale ΔT map from clocks; publish the gradient–law closure with a joint clock/AI/cavity dataset.

 doi:10.20944/preprints202511.2314.v1

2. **Propagation:** demonstrate a controlled Shapiro measurement on a terrestrial link and match the line integral of reconstructed ΔT.
3. **Cosmology:** release a baseline p fit to SN Ia+BAO+chronometers (flat prior on curvature); follow with a joint (p, Ω_{k0}) exploration and growth cross–checks.
4. **Astro scale:** publish $r_*(M)$ vs. splashback comparisons for a clean cluster subsample with environment controls.

12.7. What Would Decisively Falsify TD (in this Paper's Scope)

- A robust, coordinate–independent failure of $\mathbf{g} = -\frac{c^2}{2}\nabla\Delta T$ in the weak, quasistatic regime.
- A systematic mismatch between measured delays/deflections and the ΔT line integrals using the same mass model.
- Cosmology requiring p far from zero *while* distances and growth cannot be reconciled within Eq. (85).

13. Objections and Replies

This section anticipates common critiques and answers them within the scope and equations of this paper.

O1. "Isn't ΔT just the ADM lapse in disguise?"

Reply. Yes—in the bridge regime we set $N^2 = 1 - \Delta T$ (Eq. (47)). The novelty is *operational* and *causal*: ΔT is defined by clock ratios (Sec. 3), and TD posits an explicit space–growth clock $S(t)$ as the *cause* that, when frozen ($S \equiv c$), reproduces the GR *representation*. No extra degrees of freedom are introduced.

O2. "Then you added a scalar graviton, right?"

Reply. No. The lapse is non-dynamical in GR; reparameterizing it by ΔT does not add a propagating mode. The constraint algebra and DoF are unchanged (Sec. 8). Linearization yields the usual two tensor polarizations at speed c, with no extra scalar GW.

O3. "Local Lorentz invariance?"

Reply. Preserved. In the bridge regime $S \equiv c$ (Eq. (16)); N rescales coordinate time, not light cones. All local measurements see c; optical effects arise through the *coordinate* index $n = 1/\sqrt{1 - \Delta T}$ (Secs. 5, 9).

O4. "Equivalence principle and composition dependence?"

Reply. Universal. Test bodies couple via the single gradient law $\mathbf{g} = -\frac{c^2}{2}\nabla\Delta T$ (Eq. (10)); the source is the *active density* $\rho + (p_x + p_y + p_z)/c^2$ (Eq. (11)), i.e. the standard weak-field GR combination. No composition term appears beyond ordinary tidal effects ($\nabla\nabla\Delta T$).

O5. "$S \neq c$ constant would change physics."

Reply. With our empirical calibrations (Eq. (14)) a constant $S \neq c$ rescales gravity by S^2/c^2 (Eq. (15)). Hence the **Normalization Axiom** $S \equiv c$ (Eq. (16)). One could relabel $c \to S$ everywhere, but that is a change of units, not physics.

O6. "Why must $0 \leq \Delta T < 1$?"

Reply. Operationally, clocks do not tick faster than the baseline with normal matter sourcing. Mathematically, with asymptotic flatness and positive active density, the elliptic maximum principle gives $0 < N \leq 1$ outside horizons, hence $0 \leq \Delta T < 1$ (Sec. 2). The limit $\Delta T \to 1$ is a black boundary ($N \to 0$), not the pre-clock state $S = 0$ (Sec. 6).

 doi:10.20944/preprints202511.2314.v1

O7. "Isn't this just the Newtonian potential Φ?"

Reply. In the weak field $\Delta T \simeq 2\Phi/c^2$, so TD reduces to Newton+optics. Beyond that, ΔT is the full lapse reparameterization $N^2 = 1 - \Delta T$; strong fields and horizons are handled by N directly, not by a single scalar potential.

O8. "Gauge/coordinate dependence of ΔT?"

Reply. The *definition* uses only clock ratios and spatial differences measured along a physical baseline (Sec. 3); ΔT is an observable scalar under our stated assumptions (static exterior, chosen slicing). Coordinates are bookkeeping for maps and integrals.

O9. "Energy–momentum conservation and Bianchi identities?"

Reply. In the bridge regime the field equations and constraints are those of GR (Sec. 8); $\nabla_\mu T^{\mu\nu} = 0$ holds. In the weak, static limit our Poisson law (Eq. (11)) is the standard GR limit and is consistent with mass continuity.

O10. "Rotation (Kerr), frame dragging?"

Reply. TD maps the lapse via $N^2 = 1 - \Delta T$ while leaving the shift N^i and spatial metric γ_{ij} untouched. Frame dragging resides in N^i; Kerr observables (ISCO, lensing, redshift) are inherited slice-by-slice from GR (Sec. 8).

O11. "Gravitational waves?"

Reply. Two tensor polarizations at speed c; no extra scalar mode (Sec. 8). This is consistent with multi-messenger bounds on GW speed and polarization content.

O12. "Electromagnetic back-reaction is negligible, so why include it?"

Reply. Conceptually essential yet quantitatively tiny in labs (Sec. 7). In extreme astrophysics (e.g. magnetars) it can be a principled correction to baryonic sourcing. Propagation vs. sourcing are cleanly separated: $n(\Delta T)$ for optics; ρ_{active} for back-reaction.

O13. "Strong lensing/black hole shadow: does the index picture break?"

Reply. The isotropic-medium picture is a weak-field shorthand. Near horizons one should use the full $N^2 = 1 - \Delta T$ with the appropriate γ_{ij} (bridge to GR) to compute null geodesics. In that limit TD reproduces GR shadow/lensing predictions.

O14. "Cosmology: is $\varepsilon(t)$ distinguishable from $w(z)$?"

Reply. TD's drift yields $\Lambda(z) \propto (1+z)^{2p}$ with $w = -1$ but varying amplitude (Sec. 11). Small p is partially degenerate with (w_0, w_a) and curvature; we recommend reporting p with a clear curvature prior, then a joint (p, Ω_{k0}) analysis (Sec. 11).

O15. "Turnaround radius r_* is crude."

Reply. It is a zeroth-order, falsifiable scale from first principles: $r_* = (GM/\varepsilon^2)^{1/3}$ (Eq. (90)). Environment, tides, and infall bias the mapping to splashback/zero-velocity surfaces; we treat those as nuisances, not a failure of the anchor.

O16. "Is TD just a conformal rephrasing?"

Reply. No. TD fixes a physical normalization ($S \equiv c$) and ties observables to an operational scalar ΔT measured by clocks. The *bridge* is a field redefinition of the lapse (no new DoF), but the *cause*—a real baseline clock with possible tiny drift $\varepsilon(t)$—is additional physical content tested in Secs. 11–12.

 doi:10.20944/preprints202511.2314.v1

O17. "Inside horizons / singularities?"

Reply. This paper's domain is the exterior ($N > 0$). Horizons are $\Delta T \to 1$ surfaces; interior evolution requires a different foliation, as in GR. TD reframes the initial singularity as a *pre-clock* boundary ($S = 0$) rather than curvature blow-up; cosmological claims here are limited to homogeneous drift (Sec. 11).

O18. "Can $\Delta T < 0$ (faster clocks) occur?"

Reply. Not with normal (positive) energy under our assumptions. $\Delta T < 0$ would require exotic matter or nonstandard slicings we do not consider. With asymptotic flatness and positive active density we have $0 \leq \Delta T < 1$ (Eq. (17)).

O19. "Are your laboratory targets realistic?"

Reply. Yes. Vertical clock redshifts at the 10^{-16}/m level, AI phases $k_{\text{eff}} g T^2$, cavity shifts matching $g\,\Delta h/c^2$, and controlled Shapiro delays on engineered links are within current or near-term technology (Sec. 12). The program is falsifiable: a robust failure of $\mathbf{g} + \frac{c^2}{2}\nabla\Delta T = 0$ would refute the weak/quasistatic TD mapping.

O20. "Scope creep: where are the full dynamics?"

Reply. By design, this paper restricts to quasistatic, weak fields for clarity and testability. The full action-level bridge and constraint structure are delegated to the companion note (Sec. 8 pointer). None of the weak-field predictions used here require additional dynamics beyond the GR bridge.

14. Limitations and Scope

This paper is intentionally conservative. We isolate the minimal, operational content of TD in regimes where it can be tested cleanly, and we point to a companion bridge note for action-level details. Below we list the main assumptions, approximations, and exclusions.

14.1. Assumptions used Throughout

- **Frozen baseline in the bridge regime:** we impose the *Normalization Axiom* $S \equiv c$ (Eq. (16)) whenever we compare with GR/PPN and laboratory data.
- **Quasistatic, weak fields:** Eqs. (10), (11), (12) are used with $|\Delta T| \ll 1$ and negligible $\partial_t \Delta T$ over the measurement window.
- **Static exterior and chosen slicing:** ΔT is defined operationally for static observers (Sec. 3). Inside horizons ($N \leq 0$) we do not use ΔT; a different foliation would be required.
- **Spatially uniform drift for cosmology:** when discussing $\varepsilon(t)$ (Sec. 11) we assume it is homogeneous and small on Hubble timescales; spatial variations of S are *not* considered.

14.2. Approximations Specific to Observables

- **Optics as an isotropic medium:** the index model $n = 1/\sqrt{1-\Delta T}$ (Sec. 5) is a weak-field shorthand. Near horizons or in strong lensing we appeal to the full bridge ($N^2 = 1 - \Delta T$ with the appropriate γ_{ij}).
- **Source law:** the Poisson form (Eq. (11)) is the static, weak-field limit using the *active density* $\rho + (p_x + p_y + p_z)/c^2$. Nonlinear and time-dependent terms $\mathcal{O}(\Delta T^2)$, $\mathcal{O}(\partial_t \Delta T)$ are outside our scope.
- **Quantum tests:** Sec. 10 quantizes matter/EM on a classical background ($S \equiv c$); we do not introduce a new gravitational degree of freedom or a propagating ΔT wave.

14.3. Cosmology-Specific Caveats

- **One-parameter extension:** the $(1+z)^{2p}$ model for $\Lambda(z)$ (Eq. (84)) is a minimal ansatz; it is not a claim about the ultraviolet origin of $\varepsilon(t)$.

 doi:10.20944/preprints202511.2314.v1

- **Degeneracies:** small p is partially degenerate with curvature and (w_0, w_a); reported bounds must specify priors (Sec. 11).
- **Turnaround scale:** $r_{**} = (GM/\varepsilon^2)^{1/3}$ (Eq. (90)) is a zeroth-order anchor. Environment, tides, and infall shift observed splashback/zero-velocity radii; these are treated as nuisances, not a failure of the scaling.

14.4. What we do not *Claim Here*

- No new radiative gravitational mode; no modification of GW polarizations or speed.
- No alternative to GR in the strong-field dynamical regime; we rely on the bridge in those cases.
- No microphysical model for the "clock" or for the genesis of $S(t)$; Sec. 11 gives a phenomenological narrative only.
- No treatment of rotating/charged horizons beyond the statement that the lapse mapping recovers Kerr–Newman results slice-by-slice.

14.5. Domain of Validity (One-Line Summary)

The results in Secs. 4–12 are intended for *static/weak* fields outside horizons with $S \equiv c$ (bridge), plus a homogeneous, tiny cosmological drift $\varepsilon(t)$ that is tested against distance and growth data.

15. Conclusions

We have presented a native formulation of *Temporal Dynamics* in which a universal space–growth clock provides the *cause*, and GR emerges as the *representation* when the baseline is frozen ($S \equiv c$). A single, operational scalar—the slow–time field ΔT—controls both kinematics and optics. In the weak, quasistatic regime,

$$\mathbf{g} = -\frac{c^2}{2}\nabla\Delta T, \qquad n = \frac{1}{\sqrt{1-\Delta T}},$$

reproduce Newton's law, gravitational redshift, Shapiro delay, and light deflection; horizons are the surfaces $\Delta T \to 1$ calibrated by $D_{\mathrm{BH}} = 4GM/c^2$.

Electromagnetism on a TD background separates cleanly into *propagation* (rays/indices) and *sourcing* (active density), while quantum-ready observables follow directly from proper-time phases without adding new gravitational degrees of freedom. On cosmological scales, a tiny, homogeneous drift of the baseline, $\varepsilon(t) = \dot{S}/c$, maps to an effective $\Lambda(t) = 3\varepsilon(t)^2/c^2$, yielding a one-parameter extension of ΛCDM with falsifiable signatures in distances, growth, and the turnaround scale $r_* = (GM/\varepsilon^2)^{1/3}$.

The accompanying experimental/observational program is straightforward: map $\Delta T(\mathbf{x})$ with clock networks and verify the gradient law against gravimetry; test the optical dictionary on engineered links and lensing; and fit the cosmological extension with SN Ia, BAO, and $H(z)$, cross-checking growth. Any robust, coordinate-independent failure of these relations would falsify the framework in its stated domain.

Future directions.

(i) Present the full action-level bridge and constraint algebra; (ii) extend strong-field applications (Kerr, shadows, ringdowns) within the TD dictionary; (iii) develop a microscopic model for the clock and early-time ignition consistent with $\varepsilon(t)$; (iv) execute the cosmology fits and laboratory maps proposed here.

Takeaway.

TD articulates a cause-level picture (a real clock) whose frozen-baseline representation is GR, packages the weak-field phenomenology into one operational scalar ΔT, and offers near-term, falsifiable tests from laboratories to the Hubble scale.

Author Contributions: CRediT taxonomy. Roles follow the CRediT (Contributor Roles Taxonomy) standard. *Ogaeze Onyedikachukwu Francis (O. O. Francis):* Conceptualization; Methodology; Formal analysis; Investigation; Validation; Writing—original draft; Writing—review & editing; Visualization.

Acknowledgments: The author thanks one early reader for brief comments on clarity. This work is primarily the author's, and it builds on the existing literature in weak-field tests of GR, optical-clock metrology, gravitational lensing and time-delay formalisms, and cosmological distance–growth analyses; those contributions are acknowledged through citations throughout the text. Any remaining errors are the author's responsibility.

Funding: This work received no specific grant from any funding agency in the public, commercial, or not-for-profit sectors.

Conflicts of Interest: The author declares no competing interests.

Data Availability Statement: No new data were generated or analyzed in this study. All derivations and numerical estimates are contained in the main text and appendices; any auxiliary scripts used to produce figures will be made available upon reasonable request.

Appendix A. Units and Normalizations

Baseline (clock): $S(t)$, units $\mathrm{m\,s^{-1}}$. In the bridge regime: *Normalization Axiom* $S \equiv c$ (Eq. (16)).

Slow–time field: $\Delta T(\mathbf{x}, t) \in [0, 1)$, dimensionless. Lapse N obeys $N^2 = 1 - \Delta T$ (Eqs. (8), (47)).

Kinematics and gravity (weak/static): $v = S\,\Delta T$ and $\mathbf{g} = -(S^2/2)\,\nabla \Delta T$ (Eqs. (9), (10)). With $S \equiv c$ and $\Delta T = 2GM/(c^2 r)$, Newton's law follows.

Optics: $n(\mathbf{x}) = 1/\sqrt{1 - \Delta T(\mathbf{x})} \approx 1 + \frac{1}{2}\Delta T$ (Eq. (12)); Fermat functional $T[\Gamma] = c^{-1} \int n\, ds$.

Sourcing (weak/static): $\nabla^2 \Delta T = \frac{8\pi G}{c^2}\left(\rho + \frac{p_x + p_y + p_z}{c^2}\right)$ (Eq. (11)).

Horizon calibration: black boundary at $\Delta T = 1$; diameter $D_{\mathrm{BH}} = 4GM/c^2$ (Eq. (13)).

Sign conventions: ∇ is the flat spatial gradient in the weak field; $\hat{\mathbf{r}}$ points outward so $\partial_r \Delta T = -2GM/(c^2 r^2)$.

Appendix B. Bridge: Action Sketch and Constraints (Details)

In ADM variables (N, N^i, γ_{ij}),

$$S_{\mathrm{EH}} = \frac{c^3}{16\pi G} \int dt\, d^3x\, N\sqrt{\gamma}\left(R^{(3)} + K_{ij}K^{ij} - K^2\right) + S_{\mathrm{m}}. \tag{A1}$$

Define $\Delta T := 1 - N^2$ so $N = \sqrt{1 - \Delta T}$ and $dN/d\Delta T = -1/(2N)$. The lapse variation in TD variables is the GR Hamiltonian constraint times a nonzero factor:

$$\frac{\delta S_{\mathrm{EH}}}{\delta \Delta T} = \frac{\delta S_{\mathrm{EH}}}{\delta N}\frac{dN}{d\Delta T} = -\frac{1}{2N}\frac{\delta S_{\mathrm{EH}}}{\delta N} \;\Rightarrow\; \mathcal{H} = 0 \text{ as in GR.} \tag{A2}$$

Momentum constraints (variation of N^i) and evolution equations (variation of γ_{ij}) are unchanged; the constraint algebra and DoF therefore match GR.

Weak/static limit to the Poisson law.

Linearize around Minkowski with $N = 1 - \frac{1}{2}\Delta T$, $N^i = 0$, $\gamma_{ij} = \delta_{ij}$. The Hamiltonian constraint reduces to

$$\nabla^2 \Delta T \;=\; \frac{8\pi G}{c^2}\left(\rho + \frac{p_x + p_y + p_z}{c^2}\right), \tag{A3}$$

which is Eq. (11).

 doi:10.20944/preprints202511.2314.v1

Appendix C. PPN Snapshot ($\beta = \gamma = 1$)

With $\Delta T = 2\Phi/c^2$ (Newtonian potential Φ) and $S \equiv c$,

$$g_{tt} = -N^2c^2 = -c^2(1 - \Delta T) \approx -c^2 + 2\Phi, \tag{A4}$$

$$g_{ij} = \gamma_{ij} \;\Rightarrow\; \text{isotropic weak field } ds^2 \approx -\Big(1 - \frac{2\Phi}{c^2}\Big)c^2dt^2 + \Big(1 + \frac{2\Phi}{c^2}\Big)d\mathbf{x}^2, \tag{A5}$$

so $\gamma_{\rm PPN} = 1$. The light deflection $\hat{\alpha} = 4GM/(c^2b)$ and Shapiro delay $(2GM/c^3)\ln(\cdots)$ follow from the index $n = 1 + \Phi/c^2$ and Fermat's principle; perihelion precession reduces to the GR value with $\beta = 1$. No deviations appear in the tested weak field.

Appendix D. Kerr Note: Lapse and ΔT

In Boyer–Lindquist coordinates ($G = c = 1$ for brevity) define

$$\rho^2 = r^2 + a^2\cos^2\theta, \quad \Delta = r^2 - 2Mr + a^2, \quad A = (r^2 + a^2)^2 - a^2\Delta\sin^2\theta.$$

The 3+1 lapse for the usual Kerr foliation is

$$N \;=\; \sqrt{\frac{\rho^2\,\Delta}{A}}, \qquad \Delta T \;=\; 1 - N^2 \;=\; 1 - \frac{\rho^2\Delta}{A}. \tag{A6}$$

The shift has only a ϕ component $N^\phi = -2aMr/A$; TD leaves N^i and γ_{ij} unchanged. The black boundary occurs where $N \to 0$, i.e. $\Delta = 0$ at $r_\pm = M \pm \sqrt{M^2 - a^2}$. In the Schwarzschild limit ($a \to 0$), $N = \sqrt{1 - 2M/r}$ and $\Delta T = 2M/r$, matching the weak field $\Delta T = 2GM/(c^2r)$ and the horizon calibration.

Appendix E. Gravitational Waves: Linearization

Linearize around Minkowski with $g_{\mu\nu} = \eta_{\mu\nu} + h_{\mu\nu}$, $|h_{\mu\nu}| \ll 1$, and $N = 1 - \frac{1}{2}\Delta T$ with $|\Delta T| \ll 1$. The lapse perturbation is non-propagating (it enforces the Hamiltonian constraint). In transverse–traceless gauge the spatial metric perturbation $h_{ij}^{\rm TT}$ satisfies

$$\Box\, h_{ij}^{\rm TT} = 0, \qquad \text{phase speed } = c, \tag{A7}$$

with two tensor polarizations and no scalar mode, consistent with the bridge statement in Sec. 8.

Appendix F. Back-of-the-Envelope Numbers

Constants: $c = 2.9979 \times 10^8\ \mathrm{m\,s^{-1}}$, $G = 6.6743 \times 10^{-11}\ \mathrm{m^3\,kg^{-1}\,s^{-2}}$.
Earth: $M_\oplus = 5.972 \times 10^{24}$ kg, $R_\oplus = 6.371 \times 10^6$ m.

- **Earth surface slow–time:** $\Delta T(R_\oplus) \approx 2GM_\oplus/(c^2R_\oplus) \approx 1.4 \times 10^{-9}$.
- **Clock redshift per meter:** $\Delta\nu/\nu \approx g\,\Delta h/c^2 \approx 1.1 \times 10^{-16} \times (\Delta h/\mathrm{m})$.
- **Solar limb deflection:** $\hat{\alpha} = 4GM_\odot/(c^2R_\odot) \approx 1.75''$.
- **Solar Shapiro (grazing, one–way):** $\Delta t \sim (2GM_\odot/c^3)\ln(\cdots) \approx 120\,\mu$s.
- **Magnetar EM density:** $B \sim 10^{10}$ T $\Rightarrow u \sim B^2/(2\mu_0) \sim 4 \times 10^{25}\ \mathrm{J\,m^{-3}}$, $\rho_{\rm EM} \sim 4 \times 10^8\ \mathrm{kg\,m^{-3}}$.
- **Cosmic drift scales:** with $\varepsilon \approx H_0 \sim 2.27 \times 10^{-18}\ \mathrm{s^{-1}}$, de Sitter horizon $r_{\rm dS} = c/\varepsilon \sim 1.32 \times 10^{26}$ m (~ 4.3 Gpc). Equivalently, using $\Lambda = 3\varepsilon^2/c^2$, $r_{\rm dS} = \sqrt{3/\Lambda}$.
- **Turnaround scale:** $r_*(M) = (GM/\varepsilon^2)^{1/3}$ gives
  Sun: $\sim 3 \times 10^{18}$ m (~ 97 pc), Milky Way ($10^{12}M_\odot$): ~ 0.96 Mpc, Rich cluster ($10^{15}M_\odot$): ~ 9.6 Mpc.

Appendix G. Data-Fit Recipe for the TD Cosmology Parameter p

We fit the minimal TD extension $\varepsilon(z) = \varepsilon_0(1 + z)^p$ (Eqs. (83)–(85)).

 doi:10.20944/preprints202511.2314.v1

Inputs

SN Ia distances $\{z_i, \mu_i, \sigma_{\mu i}\}$; BAO $\{z_j, D_M(z_j)/r_d,\ H(z_j)r_d\}$; chronometer $H(z_k)$; (optional) RSD $f\sigma_8(z_\ell)$.

Model

Compute $E(z)$ from Eq. (85) with parameters $(\Omega_{m0}, \Omega_{k0}, \Omega_{\Lambda 0}, p)$ and $H(z) = H_0 E(z)$. Distances from Eqs. (86)–(88).

Likelihood (schematic)

$$\chi^2_{\rm SN} = \sum_i \frac{\left[\mu_{\rm th}(z_i;\theta) - \mu_i\right]^2}{\sigma^2_{\mu i}}, \tag{A8}$$

$$\chi^2_{\rm BAO} = \left(\mathbf{d}^{\rm th}_{\rm BAO} - \mathbf{d}^{\rm obs}_{\rm BAO}\right)^\top \mathbf{C}^{-1}_{\rm BAO} \left(\mathbf{d}^{\rm th}_{\rm BAO} - \mathbf{d}^{\rm obs}_{\rm BAO}\right), \tag{A9}$$

$$\chi^2_H = \sum_k \frac{\left[H_{\rm th}(z_k;\theta) - H(z_k)\right]^2}{\sigma^2_{Hk}}, \tag{A10}$$

with $\theta = (H_0, \Omega_{m0}, \Omega_{k0}, \Omega_{\Lambda 0}, p)$ and $\Omega_{\Lambda 0} = \varepsilon_0^2/H_0^2$. Optionally add $\chi^2_{\rm RSD}$ using Eq. (91).

Reporting

Quote p with a stated prior on Ω_{k0}; provide $p = 0$ (ΛCDM) as a nested model check. For TD key scales, report $r_*(M)$ using Eq. (90) with $\varepsilon_0 = H_0\sqrt{\Omega_{\Lambda 0}}$.

Appendix H. Notation Table

Symbol	Meaning	Units
c	Invariant local light speed; normalization baseline in bridge regime	$\mathrm{m\,s^{-1}}$
G	Newton's gravitational constant	$\mathrm{m^3\,kg^{-1}\,s^{-2}}$
$S(t)$	Space–growth clock (baseline speed)	$\mathrm{m\,s^{-1}}$
$\varepsilon(t) = \dot{S}/c$	Baseline fractional rate ("clock drift")	$\mathrm{s^{-1}}$
$\Delta T(\mathbf{x}, t)$	Slow–time field ($0 \le \Delta T < 1$)	—
N	ADM lapse, $N^2 = 1 - \Delta T$	—
N^i	ADM shift (frame dragging / rotation)	$\mathrm{m\,s^{-1}}$
γ_{ij}	Spatial 3-metric on the slice	—
$n(\mathbf{x})$	Effective refractive index, $n = 1/\sqrt{1 - \Delta T}$	—
$\mathbf{g}$	Gravitational acceleration, $-\frac{S^2}{2}\nabla\Delta T$	$\mathrm{m\,s^{-2}}$
v	Kinematic speed, $v = S\,\Delta T$ (quasistatic)	$\mathrm{m\,s^{-1}}$
ρ	Energy density divided by c^2	$\mathrm{kg\,m^{-3}}$
p_x, p_y, p_z	Principal pressures	Pa
$\rho_{\rm active}$	Active density, $\rho + (p_x + p_y + p_z)/c^2$	$\mathrm{kg\,m^{-3}}$
Φ	Newtonian potential (weak field: $\Delta T \simeq 2\Phi/c^2$)	$\mathrm{m^2\,s^{-2}}$
$H(t)$	Hubble parameter	$\mathrm{s^{-1}}$
$a(t)$	Scale factor	—
$\Lambda(t)$	Effective cosmological term, $3\varepsilon^2/c^2$	$\mathrm{m^{-2}}$
$E(z)$	Normalized expansion rate, $H(z)/H_0$	—
$\Omega_{m0}, \Omega_{r0}, \Omega_{k0}, \Omega_{\Lambda 0}$	Present-day density parameters	—

continued on next page

 doi:10.20944/preprints202511.2314.v1

Symbol	Meaning	Units
χ, D_M, D_L, D_A	Comoving, transverse comoving, luminosity, angular-diameter distances	m
$r_{\rm dS}$	de Sitter (cosmological) horizon, c/ε	m
$r_*(M)$	TD turnaround scale, $(GM/\varepsilon^2)^{1/3}$	m
r_s	Schwarzschild radius, $2GM/c^2$	m
$D_{\rm BH}$	Black-boundary diameter, $4GM/c^2$	m
b	Impact parameter (lensing/deflection)	m
$k_{\rm eff}$	Two-photon momentum transfer (atom interferometry)	m^{-1}
T	Pulse separation time in AI / interrogation time	s
ν	Clock frequency	Hz
ω	Angular frequency	s^{-1}
$u_{\rm EM}$, $\rho_{\rm EM}$	EM energy density; mass density $u_{\rm EM}/c^2$	$\mathrm{J\,m}^{-3}$; $\mathrm{kg\,m}^{-3}$

References

1. Will, C.M. The Confrontation between General Relativity and Experiment. *Living Reviews in Relativity* **2018**, *21*, 3. https://doi.org/10.1007/s41114-018-0017-9.
2. Carroll, S.M. *Spacetime and Geometry: An Introduction to General Relativity*; Addison-Wesley, 2004.
3. Wald, R.M. *General Relativity*; University of Chicago Press, 1984.
4. Schneider, P.; Ehlers, J.; Falco, E.E. *Gravitational Lenses*; Springer, 1992.
5. Francis, O.O. Temporal Dynamics: For Space–Time and Gravity. *Preprints* **2025**. Preprint, https://doi.org/10.20944/preprints202503.0453.v2.
6. Arnowitt, R.; Deser, S.; Misner, C.W. The Dynamics of General Relativity. In *Gravitation: An Introduction to Current Research*; Witten, L., Ed.; Wiley, 1962. Reprinted: Gen. Relativ. Gravit. 40, 1997–2027 (2008).
7. Gourgoulhon, E. 3+1 Formalism and Bases of Numerical Relativity, 2007, [gr-qc/0703035]. arXiv preprint.
8. Shapiro, I.I. Fourth Test of General Relativity. *Physical Review Letters* **1964**, *13*, 789–791. https://doi.org/10.1103/PhysRevLett.13.789.
9. Bertotti, B.; Iess, L.; Tortora, P. A Test of General Relativity Using Radio Links with the Cassini Spacecraft. *Nature* **2003**, *425*, 374–376. https://doi.org/10.1038/nature01997.
10. Dyson, F.W.; Eddington, A.S.; Davidson, C. A Determination of the Deflection of Light by the Sun's Gravitational Field. *Philosophical Transactions of the Royal Society A* **1920**, *220*, 291–333.
11. Abbott, B.P.; others (LIGO Scientific Collaboration.; Collaboration), V. GW170817: Observation of Gravitational Waves from a Binary Neutron Star Inspiral. *Physical Review Letters* **2017**, *119*, 161101. https://doi.org/10.1103/PhysRevLett.119.161101.
12. Abbott, B.P.; et al. Gravitational Waves and Gamma-Rays from a Binary Neutron Star Merger: GW170817 and GRB 170817A. *The Astrophysical Journal Letters* **2017**, *848*, L13. https://doi.org/10.3847/2041-8213/aa920c.
13. Francis, O.O. Temporal Dynamics as Time-First General Relativity. *Preprints* **2025**. Preprint, https://doi.org/10.20944/preprints202508.2089.v1.
14. Riess, A.G.; et al. Observational Evidence from Supernovae for an Accelerating Universe and a Cosmological Constant. *The Astronomical Journal* **1998**, *116*, 1009–1038. https://doi.org/10.1086/300499.
15. Perlmutter, S.; et al. Measurements of Ω and Λ from 42 High-Redshift Supernovae. *The Astrophysical Journal* **1999**, *517*, 565–586. https://doi.org/10.1086/307221.
16. Eisenstein, D.J.; et al. Detection of the Baryon Acoustic Peak in the Large-Scale Correlation Function of SDSS Luminous Red Galaxies. *The Astrophysical Journal* **2005**, *633*, 560–574. https://doi.org/10.1086/466512.
17. Pound, R.V.; Rebka, G.A. Apparent Weight of Photons. *Physical Review Letters* **1960**, *4*, 337–341. https://doi.org/10.1103/PhysRevLett.4.337.
18. Pound, R.V.; Snider, J.L. Effect of Gravity on Nuclear Resonance. *Physical Review Letters* **1965**, *13*, 539–540. https://doi.org/10.1103/PhysRevLett.13.539.
19. Chou, C.W.; Hume, D.B.; Koelemeij, J.C.J.; Wineland, D.J.; Rosenband, T. Optical Clocks and Relativity. *Science* **2010**, *329*, 1630–1633. https://doi.org/10.1126/science.1192720.

 doi:10.20944/preprints202511.2314.v1

20. Delva, P.; et al. Test of the Gravitational Redshift with Stable Clocks in Eccentric Orbits. *Physical Review Letters* **2018**, *121*, 231101. https://doi.org/10.1103/PhysRevLett.121.231101.
21. Herrmann, S.; et al. Test of the Gravitational Redshift with Galileo Satellites in an Eccentric Orbit. *Physical Review Letters* **2018**, *121*, 231102. https://doi.org/10.1103/PhysRevLett.121.231102.
22. Poisson, E.; Will, C.M. *Gravity: Newtonian, Post-Newtonian, Relativistic*; Cambridge University Press, 2014.
23. Francis, O.O. Essence Dynamics: Essence Interactions, Applications and Reality. Part II. *Preprints* **2024**. Preprint, https://doi.org/10.20944/preprints202409.0636.v1.
24. Ashby, N. Relativity in the Global Positioning System. *Physics Today* **2003**, *55*, 41–47. https://doi.org/10.1063/1.1485583.
25. Collaboration, E.H.T. First M87 Event Horizon Telescope Results. I. The Shadow of the Supermassive Black Hole. *The Astrophysical Journal Letters* **2019**, *875*, L1. https://doi.org/10.3847/2041-8213/ab0ec7.
26. Jackson, J.D. *Classical Electrodynamics, 3rd ed.*; Wiley, 1998.
27. Gordon, W. Zur Lichtfortpflanzung nach der Relativitätstheorie. *Annalen der Physik* **1923**, *377*, 421–456.
28. Plebański, J. Electromagnetic waves in gravitational fields. *Phys. Rev.* **1960**, *118*, 1396–1408.
29. Kasevich, M.; Chu, S. Atomic interferometry using stimulated Raman transitions. *Phys. Rev. Lett.* **1991**, *67*, 181–184.
30. Cronin, A.D.; Schmiedmayer, J.; Pritchard, D.E. Optics and interferometry with atoms and molecules. *Rev. Mod. Phys.* **2009**, *81*, 1051–1129.
31. Hogg, D.W. Distance measures in cosmology. *arXiv:astro-ph/9905116* **1999**.
32. Pavlidou, V.; Tomaras, T.N. Where the world stands still: turnaround radius in ΛCDM. *JCAP* **2014**, *09*, 020.
33. Dodelson, S. *Modern Cosmology*; Academic Press, 2003.
34. Linder, E.V. Cosmic Growth History and Expansion History. *Physical Review D* **2005**, *72*, 043529. https://doi.org/10.1103/PhysRevD.72.043529.
35. Moresco, M.; et al. Improved Constraints on the Expansion Rate of the Universe up to z $\sim$ 1.1 from the Spectroscopic Evolution of Cosmic Chronometers. *JCAP* **2012**, *2012*, 006. https://doi.org/10.1088/1475-7516/2012/08/006.
36. Collaboration, P. Planck 2018 results. VI. Cosmological parameters. *A&A* **2020**, *641*, A6.